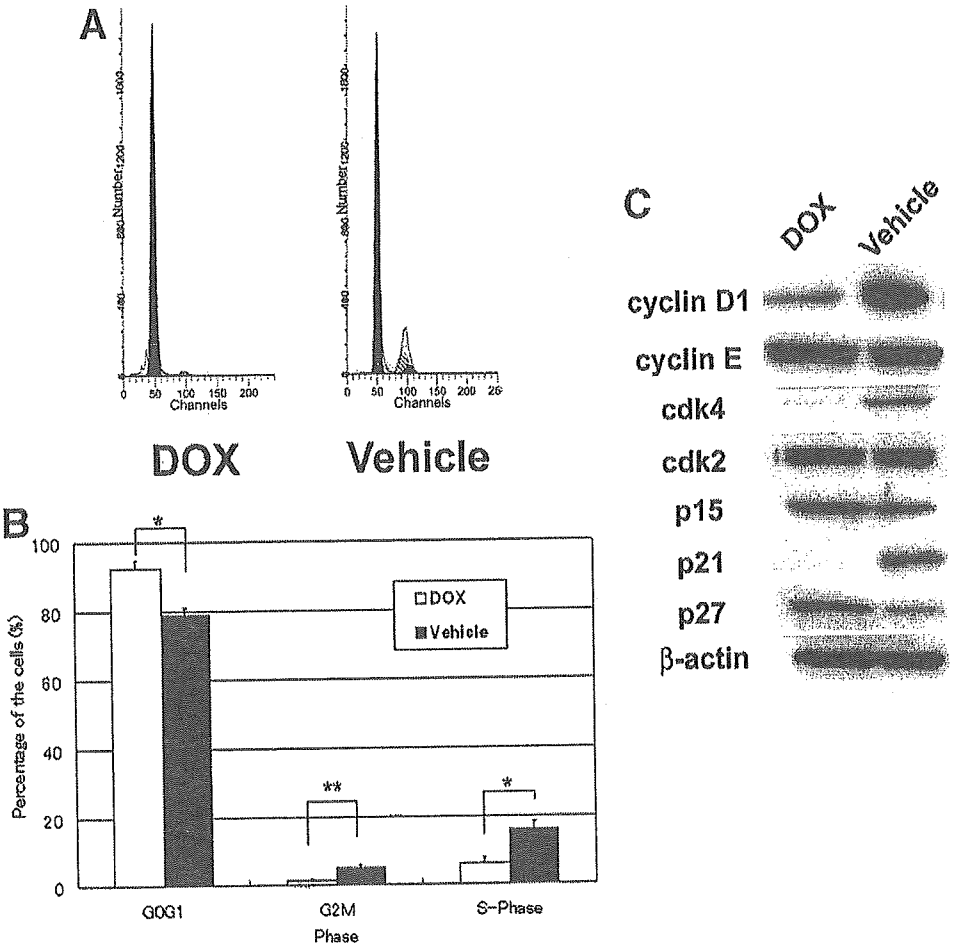

Figure 4. tICAMEK-expressing cells are resistant to NaB-mediated cell cycle arrest. (*A*) Cell cycle analysis of RIE-tiCAMEK cells with DOX (no CA-MEK expression) or vehicle (CA-MEK expression) at 72 hours after treatment with NaB (5 mmol/L). (*B*) Results from *A* expressed as percentage of cells in each stage of the cell cycle. Values are the means ± SE of 3 separate experiments. $*P < .005$, $**P < .001$. (*C*) Western blot analysis of cyclin D1, cyclin E, cdk4, cdk2, p15, $p21^{Cip/WAF1}$, and $p27^{Kip}$ expression in RIE-tiCAMEK cells (with DOX or vehicle) following treatment with NaB for 72 hours.

cCAMEK and IEC-Mock cells (data not shown). COX-2 induction was confirmed by Northern blot analysis in RIE-tiCAMEK cells following the removal of DOX (Figure 5*D*). Therefore, increased levels of COX-2 accompanied by an increase in PGE_2 and PGI_2 may contribute to the antiapoptotic properties of CA-MEK.

To determine the involvement of ERK activation in the expression of COX-2, we established RIE-tiCAMEK cells with dominant negative ERK1 or 2 expression vectors. Western blot analysis shows that the overexpression of dominant negative ERK1 or 2 inhibits the expression of COX-2 in RIE-tiCAMEK cells (Figure 5*E*). This result confirms that ERK activity is involved in the CA-MEK–induced expression of COX-2.

Regulation of COX-2 in CA-MEK–Expressing Cells

To determine the mechanisms by which COX-2 expression is regulated in CA-MEK–expressing cells following treatment with NaB, we examined transcriptional and posttranscriptional regulation of the *COX-2* gene. Due to the internal expression of luciferase of RIE-tiCAMEK cells, we used RIE-cCAMEK and RIE-Mock cells for this study. A series of human *COX-2* promoter deletion constructs was transfected into RIE-cCAMEK and RIE-Mock cells. The transcriptional activity was increased in RIE-cCAMEK cells compared with RIE-Mock cells. The highest transcriptional activity was found with the full-length (−1432/+59) promoter construct (Figure 6*A*). Removal of the 2 nuclear factor κB sites, the upstream (−327/+59) and the downstream (−220/+59), or deletion of both the nuclear factor/interleukin-6 site (−124/+59) and the CRE (−52/+59) elements resulted in decreased transcriptional activity of COX-2. Mutating the CRE and/or nuclear factor/interleukin-6 site also reduced the transcriptional activity.

Posttranscriptional regulation via stabilization of COX-2 mRNA plays an important role in the regulation of COX-2 levels in a variety of cultured cells.[62] As shown in Figure 6*B* and *C*, COX-2 mRNA was rapidly degraded in RIE-tiCAMEK cells treated with DOX (half-life, <15 minutes). However, CA-MEK expression

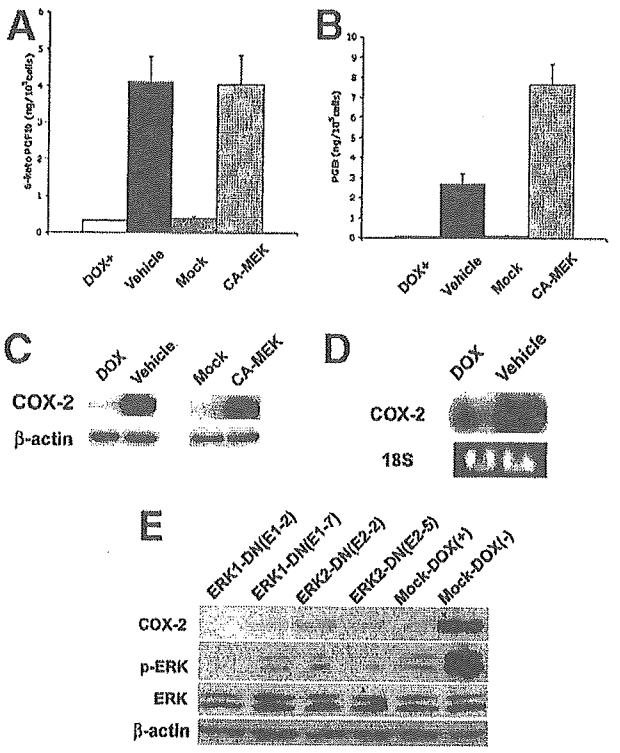

Figure 5. PG production and COX-2 expression following treatment with NaB. (*A*) 6-keto $PGF_{1\alpha}$ and (*B*) PGE_2 production at 48 hours after treatment with NaB in RIE-tiCAMEK cells with 2 μg/mL DOX (no CA-MEK expression) or vehicle (CA-MEK expression), RIE-Mock cells, and RIE-cCAMEK cells. Values are the means ± SE of 3 separate experiments performed in triplicate. (*C*) Western blot analysis of COX-2 at 48 hours following treatment with NaB in RIE-tiCAMEK cells (with 2 μg/mL DOX or vehicle), RIE-mock cells, and RIE-cCAMEK cells. (*D*) Northern blot analysis of COX-2 in tiCAMEK-expressing RIE cells with 2 μg/mL DOX or vehicle at 48 hours following treatment with NaB. (*E*) Sequential transfected RIE-tiCAMEK cells with ERK1 dominant negative vector or ERK2 dominant negative vector were established. Western blot analysis shows the expression levels of COX-2, phosphorylated ERK (p-ERK), ERK, and β-actin in the cells. ERK1 dominant negative clones (ERK1-DN; clone E1-2 and E1-7), ERK2 dominant negative clones (ERK2-DN; clone E2-2 and E2-5), and empty vector (pCEP4) transfected RIE-tiCAMEK cells (Mock) with or without DOX are shown.

markedly increased the stability of COX-2 mRNA and extended the half-life >60 minutes. These results indicated a marked increase in mRNA stability following MEK1 activation.

Pharmacologic Inhibition of COX-2 Inhibits MEK-Dependent Tumor Growth In Vivo by Stimulating Apoptosis

Overexpression of COX-2 frequently occurs in a variety of human malignancies, including those of colon, lung, breast, skin, and esophagus.[32] We have shown that COX-2 is strongly expressed in MEK-transformed cells and may induce antiapoptotic properties. To verify this hypothesis in vivo, we treated mice xenografted with IEC-cCAMEK cells and RIE-cCAMEK cells with a COX-2–selective inhibitor (celecoxib) and evaluated the growth rate of MEK-induced tumors. As shown in Figure 7*A*, treatment of IEC-cCAMEK xenografted mice with celecoxib for 17 days induced a 72% reduction in tumor volume when compared with vehicle-treated controls. A similar inhibitory effect was also found with celecoxib-treated RIE-cCAMEK (clone DD14) tumors, although to a lesser extent (Figure 7*A*). Western blot analysis of tissues from the excised tumors showed that the expression of Bcl-X_L was decreased in the celecoxib-treated mice (Figure 7*B*). Moreover, increased apoptotic staining was seen in the celecoxib-treated tissues. We observed 0.7 ± 0.3 apoptotic IECcCAMEK(D1) cells per field in untreated mice (vehicle) and 5.9 ± 2.1 apoptotic IECcCAMEK(D1) cells per field in celecoxib-treated mice (Figure 7*C*). Similarly, we found 1.2 ± 0.5 apoptotic RIEcCAMEK(DD14) cells per field in untreated mice (vehicle) and 5.1 ± 1.7 apoptotic RIEcCAMEK(DD14) cells per field in celecoxib-treated mice (Figure 7*C*). Therefore, the in vivo effects of celecoxib on tumor volume may also occur through the inhibition of the antiapoptotic properties of COX-2, including the down-regulation of Bcl-X_L.

Discussion

Here we show that CA-MEK1 transforms both RIE-1 and IEC-6 rat intestinal epithelial cells. This finding is in agreement with a recent report showing the ability of CA-MEK to transform IEC-6 cells.[24] However, Oldham et al[23] reported that constitutively active mutants of Raf-1 did not transform RIE-1 and IEC-6 cells. This finding shows key differences between the Raf-1 and CA-MEK signaling cascades in intestinal epithelial cells. Recent evidence shows that Raf-1 may use multiple effectors other than MEK-ERK to mediate its cellular effects. For example, activated Raf-1, but not MEK, can drive the differentiation of hippocampal neuronal cells, whereas mutant Raf-1, defective in MEK activation, is still capable of activating selected signaling pathways.[63,64] Although Raf-1 activates MEK1, these observations suggest a significant difference between downstream signals affected by the activation of Raf-1 and MEK1 pathways.

In this study, we show that MEK-ERK signaling can protect against NaB-mediated apoptosis. Several reports provide evidence that the MEK-ERK pathway has been implicated in protection from various proapoptotic signals via modulation of antiapoptotic proteins such as Bcl-X_L, Bcl-2, and Mcl-1.[10–14] Our results suggest that the CA-MEK signal up-regulates the expression of Bcl-

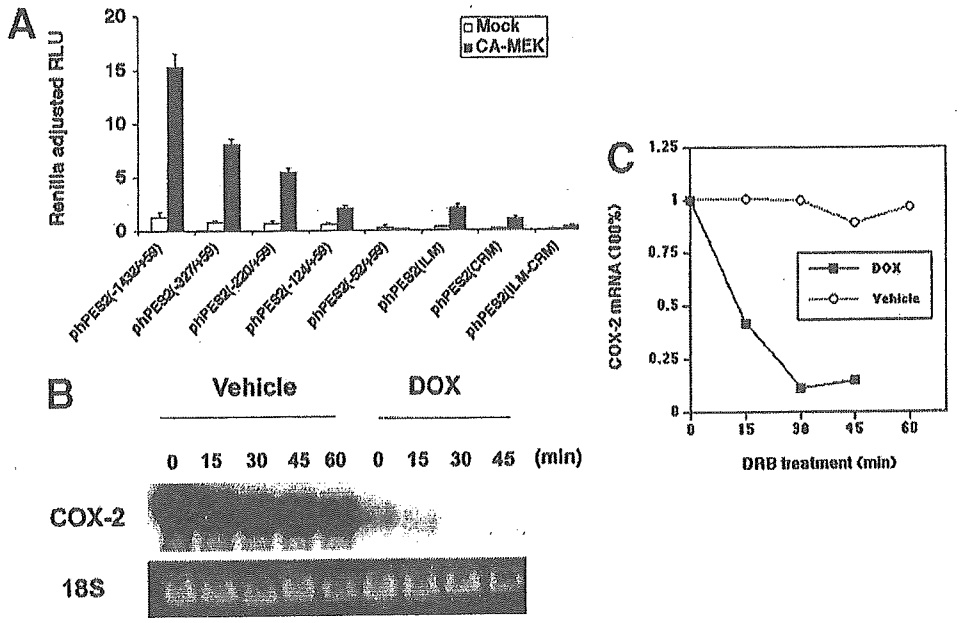

Figure 6. COX-2 regulation in CA-MEK cells following treatment with NaB. (*A*) COX-2 promoter assay using cCAMEK-expressing RIE cells compared with the mock-transfected cells at 24 hours after treatment with NaB are shown. The values are shown as *Renilla* adjusted luciferase values and represent the average ± SD of 3 independent experiments performed in quadruplicate. (*B*) Northern blot analysis of COX-2 mRNA in tiCAMEK-expressing RIE cells with and without DOX. RIE-tiCAMEK cells with DOX or vehicle were treated with 5 mmol/L NaB for 24 hours. Further transcriptional activity was blocked by the addition of 100 μmol/L of 5,6-dichlorobenzimidazole riboside. Total RNA samples were isolated at the indicated times and probed with a labeled COX-2 complementary DNA probe. (*C*) The results from *B* were analyzed by densitometry scanning using the Scion Image program and normalized by 18S.

X_L, Mcl-1, and COX-2. Previously, we have shown that forced expression of COX-2 leads to the inhibition of apoptosis in intestinal epithelial cells.[34] Therefore, COX-2 may play an important role in MEK-associated resistance to apoptosis. We observed an increased rate of apoptosis and decreased levels of Bcl-X_L in the MEK-induced tumors. Other groups have reported that the treatment of APC^{min} mice with a COX-2–selective inhibitor resulted in increased apoptosis and a reduction of Bcl-X_L levels in adenomatous polyps.[65] Additionally, Mcl-1 is also regulated via COX-2 signaling. Mcl-1 levels are tightly regulated by COX-2 in human lung adenocarcinoma cells and contribute to cell survival.[66] Therefore, the regulation of these antiapoptotic proteins may be linked to the expression of COX-2. Conversely, phosphorylation of Bad on Ser^{112} or Ser^{136} dissociates Bcl-X_L/Bad heterodimers and unmasks the antiapoptotic effect of Bcl-X_L.[54,58] Therefore, increased phosphorylation of Bad (Ser^{112}) may also act as a negative regulator of apoptosis in CA-MEK–expressing cells. Collectively, elevated expression of antiapoptotic Bcl-X_L, Mcl-1, and COX-2, reduced expression of the proapoptotic protein Bak, and inhibition of the proapoptotic effect of Bad may all contribute to the antiapoptotic effects of CA-MEK–expressing cells.

Cell cycle progression is another important aspect of tumorigenesis. Abnormalities in the expression of cell-cycle regulatory proteins have been reported in tumors of the small bowel and in colorectal carcinomas.[67] We show here that MEK activation leads to elevated levels of cyclin D1 and cdk4 and decreased levels of $p27^{Kip}$ expression that may confer resistance to NaB-mediated cell cycle arrest. Furthermore, we did not observe any changes in cyclin E or cdk2 expression. Similar findings were published by Boucher et al,[24] who showed that cyclin D1, cdk2, and cdk4 proteins were increased and $p27^{Kip}$ was decreased in CA-MEK–expressing IEC-6 cells. Additionally, another report shows that the activation of the MAPK cascade was required for S-phase entry and $p27^{Kip}$ down-regulation in IEC-6 cells.[68] Therefore, the activation of the MEK pathway may contribute to cell G_0/G_1 progression via cyclin D1 and cdk4 as well as S-phase entry by down-regulating $p27^{Kip}$, at least in rodent immortalized intestinal cells. In contrast to the forced mitogenesis of CA-MEK–expressing IEC-6 cells, Boucher et al[24] also showed CA-MEK–induced cell cycle arrest in nonimmortalized human intestinal epithelial cells by up-regulating $p21^{Cip/WAF1}$, p53, and p16 expression. They suggested that the noninduction of $p21^{Cip/WAF1}$, p53, and p16 in CA-MEK–expressing

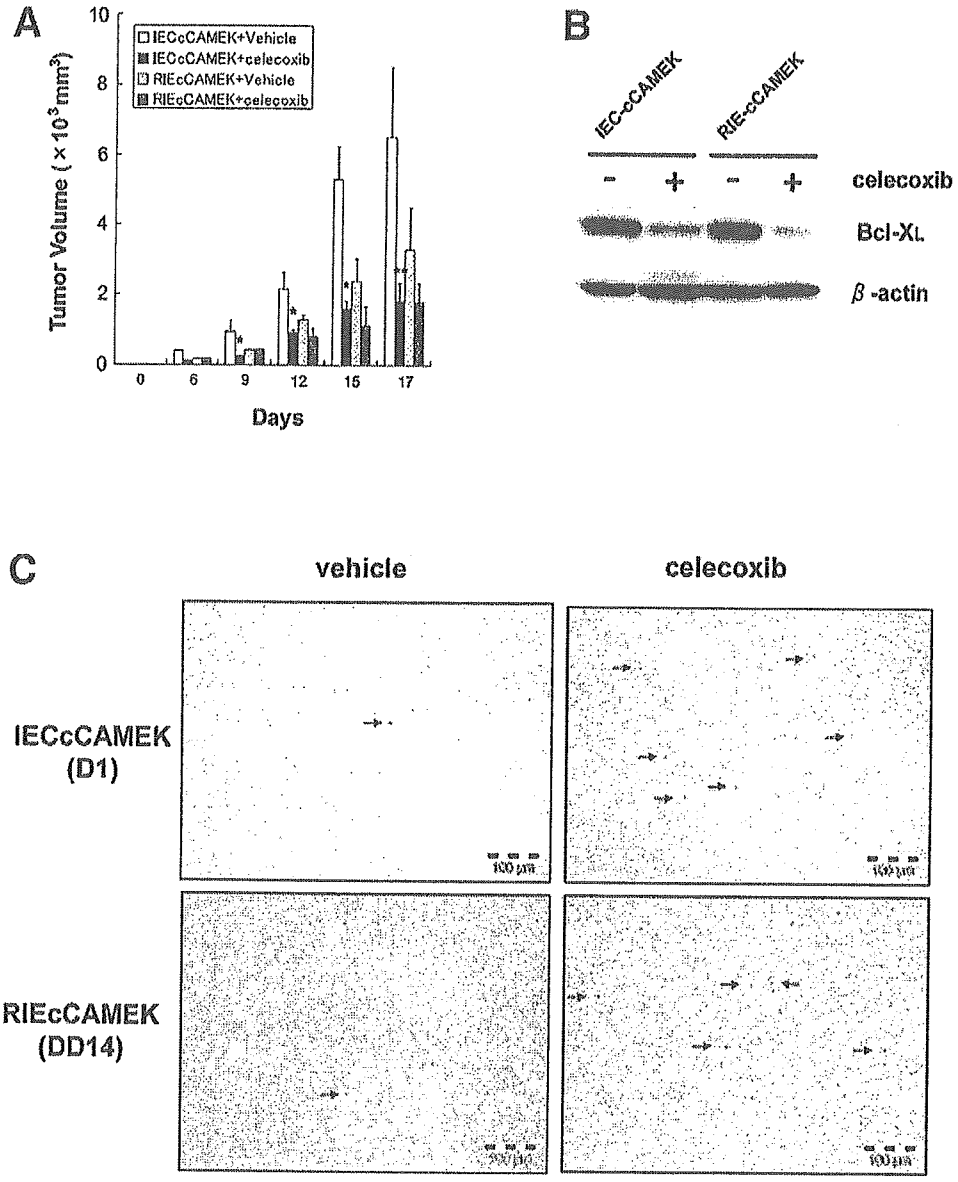

Figure 7. Pharmacologic inhibition of COX-2 reduces cCAMEK-expressing tumor growth in vivo. (*A*) A total of 1×10^6 IEC-cCAMEK (clone D1) and RIE-cCAMEK (clone DD14) cells suspended in 0.2 mL DMEM were injected into the dorsal subcutaneous tissue of athymic nude mice. Mice were given a COX-2–selective inhibitor (celecoxib, 100 mg/kg) (n = 3 mice per each group; n = 3 mice in the RIE-cCAMEK injected group) or vehicle (n = 3 mice per each group) by daily gavage, and the treatment was continued for 17 days. Tumor volumes were calculated from measurements taken at the indicated times and calculated using the following formula: $V = L \times W^2 \times 0.5$, where *V* is volume, *L* is length, and *W* is width. Data are represented as the average of each group ± SD. $*P < .05$, $**P < .01$ vs vehicle-treated control. (*B*) Western blot analysis of tissues from IEC-cCAMEK (clone D1) and RIE-cCAMEK (clone DD14) tumors. β-actin indicates equal protein loaded in each lane. (*C*) Terminal deoxynucleotidyl transferase–mediated deoxyuridine triphosphate nick-end labeling staining of IEC-cCAMEK (D1) and RIE-cCAMEK (DD14) tissue sections. *Arrows* indicate brown-stained apoptotic cells.

IEC-6 cells may contribute to these differences. However, we find that $p21^{Cip/WAF1}$, a universal inhibitor of cyclin-dependent kinases, was increased in CA-MEK–transformed cells. Here, we show that CA-MEK–expressing RIE cells were resistant to NaB-mediated cell cycle arrest and apoptosis despite the up-regulation of $p21^{Cip/WAF1}$. $p21^{Cip/WAF1}$ is also reported to act as an adaptor protein to promote assembly of the active cdk4/cyclinD1 complex,[69] and the forced expression of cyclin D1 in human glioma and rodent fibroblast cells induced $p21^{Cip/WAF1}$ expression without altering cell cycle progression.[70] Moreover, recent studies have shown that $p21^{Cip/WAF1}$ can act as an antiapoptotic and growth-promoting protein in addition to its known growth inhibitory role.[71–73] The overexpression of $p21^{Cip/WAF1}$ is an early event in the development of some neoplasms, and $p21^{Cip/WAF1}$ is currently being evaluated as a therapeutic cancer target.[61,74] Therefore, we speculate that the increase of $p21^{Cip/WAF1}$ following MEK activation may have an antiapoptotic and growth-promoting role, at least in this context.

We have clearly shown that the activation of MEK signaling alone is sufficient to induce COX-2 in rat intestinal epithelial cells at both transcriptional and posttranscriptional levels. Therefore, COX-2–derived bioactive lipids may play a key role in tumor formation via activating the MEK-ERK cascade. Surprisingly, CA-MEK–expressing cells produce not only PGI_2 but also PGE_2. These cells do not normally produce PGE_2,[45] but PGE_2 levels are increased in human colon cancer tissue

compared with surrounding normal mucosa.[75] PGE_2 has also been reported to inhibit programmed cell death and enhance invasiveness of colorectal carcinoma cells.[76] Furthermore, PGE_2 can activate epidermal growth factor receptor,[77] which leads to ERK activation and can trigger ERK2-mitogenic signaling in gastric epithelial and colon carcinoma cells.[78]

We show that the expression of CA-MEK results in the transformation of rat intestinal epithelial cells and that activation of the MEK-ERK cascade suppresses programmed cell death and leads to tumorigenesis. COX-2 may also play an important role in MEK-induced tumor formation through stimulation of resistance to apoptosis. These results also indicate that the MEK-ERK signaling pathway may provide an important target for developing new cancer drugs. We suspect that MEK-ERK kinase inhibitors are currently being developed for clinical use.

References

1. Green DR, Evan GI. A matter of life and death. Cancer Cell 2002;1:19–30.
2. Seger R, Krebs EG. The MAPK signaling cascade. FASEB J 1995; 9:726–735.
3. Kyriakis JM, Avruch J. Sounding the alarm: protein kinase cascades activated by stress and inflammation. J Biol Chem 1996; 271:24313–24316.
4. Wilkinson MG, Millar JBA. Control of the eukaryotic cell cycle by MAP kinase signaling pathways. FASEB J 2000;14:2147–2157.
5. Robinson MJ, Cobb MH. Mitogen-activated protein kinase pathways. Curr Opin Cell Biol 1997;9:180–186.
6. Babyastsky MW, Podolsky DK. Growth and development of the gastrointestinal tract. In: Yamada T, ed. Textbook of gastroenterology. Volume 1. 3rd ed. Philadelphia, PA: JB Lippincott, 1999: 547–584.
7. Taupin D, Podolsky DK. Mitogen-activated protein kinase activation regulates intestinal epithelial differentiation. Gastroenterology 1999;116:1072–1080.
8. Aliaga JC, Deshenes C, Beaulieu J-F, Calvo EL, Rivard N. Requirement of the MAP kinase cascade for cell cycle progression and differentiation of human intestinal cells. Am J Physiol 1999;277: G631–G641.
9. Ding Q, Wang Q, Evers BM. Alterations of MAPK activities associated with intestinal cell differentiation. Biochem Biophys Res Commun 2001;284:282–288.
10. Boucher M-J, Morisset J, Vachon PH, Reed JC, Laine J, Rivard N. MEK/ERK signaling pathway regulates the expression of Bcl2, Bcl-XL, and Mcl-1 and promotes survival of human pancreatic cancer cells. J Cell Biochem 2000;79:355–369.
11. Jost M, Huggett TM, Kari C, Boise LH, Rodeck U. Epidermal growth factor receptor-dependent control of keratinocyte survival and Bcl-X_L expression through a MEK-dependent pathway. J Biol Chem 2001;276:6320–6326.
12. Bryckaert M, Guillonneau X, Hecquet C, Courtois Y, Mascarelli F. Both FGF1 and Bcl-X synthesis are necessary for the reduction of apoptosis in retinal pigmented epithelial cells by FGF2: role of the extracellular signal-regulated kinase 2. Oncogene 1999;18:7584–7593.
13. Pardo OE, Arcaro A, Salerno G, Raguz S, Downward J, Seckl MJ. Fibroblast growth factor-2 induces transcriptional regulation of Bcl-X_L and Bcl-2 via a MEK-dependent pathway. J Biol Chem 2002;277:12040–12046.
14. Townsend KJ, Trusty JL, Traupman MA, Eastman A, Craig RW. Expression of the antiapoptotic MCL1 gene product is regulated by a mitogen activated protein kinase-mediated pathway triggered through microtubule disruption and protein kinase C. Oncogene 1998;17:1223–1234.
15. Bos JL. Ras oncogene in human cancer: a review. Cancer Res 1989;49:4682–4689.
16. Davis H, Bignell GR, Cox C, Stephens P, Edkins S, Clegg S, Teague J, Woffendin H, Garnett MJ, Bottomley W, Davis N, Dicks E, Ewing R, Floyd Y, Gray K, Hall S, Hawes R, Hughes J, Kosmidou V, Menzies A, Mould C, Parker A, Stevens C, Watt S, Hooper S, Wilson R, Jayatilake H, Gusterson BA, Cooper C, Shipley J, Hargrave D, Pritchard-Jones K, Maitland N, Chenevix-Trench G, Riggins GJ, Bigner DD, Palmieri G, Cossu A, Flanagan A, Nicholson A, Ho JW, Leung SY, Yuen ST, Weber BL, Seigler HF, Darrow TL, Paterson H, Marais R, Marshall CJ, Wooster R, Stratton MR, Futreal PA. Mutations of the BRAF gene in human cancer. Nature 2002;417:949–954.
17. Hoshino R, Chatani Y, Yamori T, Tsuruo T, Oka H, Yoshida O, Shimada Y, Ari-i S, Wada H, Fujimoto J, Kohno M. Constitutive activation of the 41-/43-kDa mitogen-activated protein kinase signaling pathway in human tumors. Oncogene 1999;18:813–822.
18. Licato LL, Brenner DA. Analysis of signaling protein kinases in human colon or colorectal carcinomas. Dig Dis Sci 1998;43: 1454–1464.
19. Kuno Y, Kondo K, Iwata H, Senga T, Akiyama S, Ito K, Takagi H, Hamaguchi M. Tumor-specific activation of mitogen-activated protein kinase in human colorectal and gastric carcinoma tissues. Jpn J Cancer Res 1998;89:903–909.
20. Lee SH, Lee JW, Soung YH, Kim SY, Nam SW, Park WS, Kim SH, Yoo NJ, Lee JY. Colorectal tumors frequently express phosphorylated mitogen-activated protein kinase. APMIS 2004;112:233–238.
21. Eggstein P, Franke M, Kutschka I, Manthey G, von Specht BU, Ruf G, Farthmann EH. Expression and activity of mitogen activated protein kinases in human colorectal carcinoma. Gut 1999;44: 834–838.
22. Wang Q, Ding Q, Dong Z, Ehlers RA, Evers BM. Downregulation of mitogen-activated protein kinases in human colon cancers. Anticancer Res 2000;20:75–83.
23. Oldham SM, Clark GJ, Gangarosa LM, Coffey RJJ, Der CJ. Activation of the Raf-1/MAP kinase cascade is not sufficient for Ras transformation of RIE-1 epithelial cells. Proc Natl Acad Sci U S A 1996;93:6924–6928.
24. Boucher M-J, Jean D, Vezina A, Rivard N. Dual role of MEK/ERK signaling in senescence and transformation of intestinal epithelial cells. Am J Physiol 2004;286:G736–G746.
25. Taniura S, Nomura K, Ozaki K-I, Tsujimoto M, Kondo T, Kohno M. Prolonged nuclear retention of activated extracellular signal-regulated kinase 1/2 is required for hepatocyte growth factor-induced cell motility. J Biol Chem 2002;277:28256–28264.
26. Taniura S, Asato K, Fujishiro S-H, Kohno M. Specific blockade of the ERK pathway inhibits the invasiveness of tumor cells: down-regulation of matrix metalloproteinase-3/-9/-14 and CD44. Biochem Biophys Res Commun 2003;304:801–806.
27. Hoshino R, Taniura S, Watanabe K, Kataoka T, Kohno M. Blockade of the extracellular signal-regulated kinase pathway induces marked G1 cell cycle arrest and apoptosis in tumor cells in which the pathway is constitutively activated. Up-regulation of p27Kip1. J Biol Chem 2001;276:2686–2692.
28. Milanini J, Vinals F, Pouyssegur J, Pages G. p42/p44 MAP kinase module plays a key role in the transcriptional regulation of the vascular endothelial growth factor gene in fibroblasts. J Biol Chem 1998;273:18165–18172.
29. MacKeigan JP, Collins TS, Ting J-Y. MEK inhibition enhances paclitaxel-induced tumor apoptosis. J Biol Chem 2000;275:38953–38956.

30. Dent P, Grant S. Pharmacologic interruption of the mitogen-activated extracellular regulated kinase/mitogen-activated protein kinase signal transduction pathway: potential role in promoting cytotoxic drug action. Clin Cancer Res 2001;7:775–783.
31. Sebolt-Leopold JS, Dudley DT, Herrera R, Van Becelaere K, Wiland A, Gowan RC, Tecle H, Barrett SD, Bridges A, Przybranowski S, Leopold WR, Saltiel AR. Blockage of the MAP kinase pathway suppresses growth of colon tumors in vivo. Nat Med 1999;5:810–816.
32. Gupta RA, DuBois RN. Colorectal cancer prevention and treatment by inhibition of cyclooxygenase-2. Nat Rev Cancer 2001;1:11–21.
33. Kawai N, Tsujii M, Tsuji S. Cyclooxygenases and colon cancer. Prostaglandins Other Lipid Mediat 2002;68-69:187–196.
34. Tsujii M, DuBois RN. Alterations in cellular adhesion and apoptosis in epithelial cells overexpressing prostaglandin endoperoxide synthase 2. Cell 1995;83:493–501.
35. Subbaramiah K, Telang N, Ramonetti JT, Araki R, DeVito B, Weksler BB, Dannenberg AJ. Transcription of cyclooxygenase-2 is enhanced in transformed mammary epithelial cells. Cancer Res 1996;56:4424–4429.
36. Heasley LE, Thaler S, Nicks M, Price B, Skorecki K, Nemenoff RA. Induction of cytosolic phospholipase A2 by oncogenic Ras in human non-small cell lung cancer. J Biol Chem 1997;272:14501–14504.
37. Sheng H, Williams CS, Shao J, Liang P, DuBois RN, Beauchamp RD. Induction of cyclooxygenase-2 by activated Ha-*ras* oncogene in Rat-1 fibroblasts and the role of Mitogen-activated protein kinase. J Biol Chem 1998;273:22120–22127.
38. Sheng H, Shao J, DuBois RN. K-Ras-mediated increase in cyclooxygenase 2 mRNA stability involves activation of the protein kinase B. Cancer Res 2001;61:2670–2675.
39. DuBois RN, Tsujii M, Bishop P, Awad JA, Makita K, Lanahan A. Cloning and characterization of a growth factor-inducible cyclooxygenase gene from rat intestinal epithelial cells. Am J Physiol 1994;266:G822–G827.
40. Huang W, Kessler DS, Erikson RL. Biochemical and biological analysis of Mek1 phosphorylation site mutants. Mol Biol Cell 1995;6:237–245.
41. Sheng H, Shao J, DuBois RN. Akt/PKB activity is required for Ha-Ras-mediated transformation of intestinal epithelial cells. J Biol Chem 2001;276:14498–14504.
42. Wang J, Sun LZ, Myeroff L, Wang X, Gentry LE, Yang J, Liang J, Zborowska E, Markowitz S, Willson JKV, Brattain MG. Demonstration that mutation of the Type II transforming growth factor beta receptor inactivates its tumor suppressor activity in replication error-positive colon carcinoma cells. J Biol Chem 1995;270:22044–22049.
43. Reese J, Zhao X, Ma W-G, Brown N, Maziasz TJ, Dey SK. Comparative analysis of pharmacologic and/or genetic disruption of cyclooxygenase-1 and cyclooxygenase-2 function in female reproduction in mice. Endocrinology 2001;142:3198–3206.
44. Freshney RI. Culture of animal cells: a manual of basic technique. 4th ed. New York, NY: Wiley-Liss, 2000.
45. DuBois RN, Awad J, Morrow J, Roberts LJI, Bishop PR. Regulation of eicosanoid production and mitogenesis in rat intestinal epithelial cells by transforming growth factor-alpha and phorbol ester. J Clin Invest 1994;93:493–498.
46. Shao J, Sheng H, Inoue H, Morrow JD, DuBois RN. Regulation of constitutive cyclooxygenase-2 expression in colon carcinoma cells. J Biol Chem 2000;275:33951–33956.
47. Zhang Z, Sheng H, Shao J, Beauchamp RD, DuBois RN. Posttranscriptional regulation of cyclooxygenase-2 in rat intestinal epithelial cells. Neoplasia 2000;2:523–530.
48. Yan M, Templeton DJ. Identification of 2 serine residues of MEK-1 that are differentially phosphorylated during activation by raf and MEK kinase. J Biol Chem 1994;269:19067–19073.
49. Alessandrini A, Greulich H, Huang W, Erickson RL. Mek1 phosphorylation site mutants activate Raf-1 in NIH3T3 cells. J Biol Chem 1996;271:31612–31618.
50. Gossen M, Bujard H. Tight control of gene expression in mammalian cells by tetracycline responsive promoters. Proc Natl Acad Sci U S A 1992;89:5547–5551.
51. Diaz C, Schroit AJ. Role of translocases in the generation of phosphatidylserine asymmetry. J Membr Biol 1996;151:1–9.
52. Engeland VM, Nieland LJW, Ramaekers FCS, Schutte B, Reutelingsperger CPM. Annexin V-affinity assay: a review on an apoptosis detection system based on phosphatidylserine exposure. Cytometry 1998;31:1–9.
53. Adams JM, Cory S. The Bcl-2 protein family: arbiters of cell survival. Science 1998;281:1322–1326.
54. Zha J, Harada H, Yang E, Jockel J, Korsmeyer SJ. Serine phosphorylation of death agonist BAD in response to survival factor results in binding to 14-3-3 not BCL-XL. Cell 1996;87:619–628.
55. Datta SR, Dudek H, Tao X, Masters S, Fu H, Gotoh Y, Greenberg ME. Akt phosphorylation of BAD couples survival signals to the cell-intrinsic death machinery. Cell 1997;91:231–241.
56. Peso LD, Gonzalez-Gracia M, Page C, Herrera R, Nunez G. Interleukin-3-induced phosphorylation of BAD through the protein kinase Akt. Science 1997;278:687–689.
57. Bonn A, Brunet A, West AE, Datta R, Takasu MA, Greenberg ME. Cell survival promoted by the Ras-MAPK signaling pathway by transcription-dependent and -independent mechanisms. Science 1999;286:1358–1362.
58. Scheid MP, Schubert KM, Duronio V. Regulation of Bad phosphorylation and association with Bcl-xL by the MAPK/Erk kinase. J Biol Chem 1999;274:31108–31113.
59. Davis RJ. Signal transduction by the JNK group of MAP kinases. Cell 2000;103:239–252.
60. Kandel ES, Hay N. The regulation and activities of the multifunctional serine/threonine kinase Akt/PKB. Exp Cell Res 1999;253:210–229.
61. Weiss RH. $p21^{Waf1/Cip1}$ as a therapeutic target in breast and other cancers. Cancer Cell 2003;4:425–429.
62. Sheng H, Shao J, Dixon DA, Williams CS, Prescott SM, DuBois RN, Beauchamp RD. Transforming growth factor-α1 enhances Ha-ras-induced expression of cyclooxygenase-2 in intestinal epithelial cells via stabilization of mRNA. J Biol Chem 2000;275:6628–6635.
63. Kuo WL, Abe M, Rhee J, Eves EM, McCarthy SA, Yan M, Templeton DJ, McMahon M, Rosner MR. Raf, but not MEK or ERK, is sufficient for differentiation of hippocampal neuronal cells. Mol Cell Biol 1996;16:1458–1470.
64. Pearson G, Bumeister R, Henry DO, Cobb MH, White MA. Uncoupling Raf1 from MEK1/2 impairs only a subset of cellular responses to Raf activation. J Biol Chem 2000;275:37303–37306.
65. Sunayama K-I, Konno H, Nakamura T, Kashiwabara H, Shoji T, Tsuneyoshi T, Nakamura S. The role of cyclooxygenase-2 (COX-2) in two different morphological stages of intestinal polyps in APC^{474} knockout mice. Carcinogenesis 2002;23:1351–1359.
66. Lin M-T, Lee R-C, Yang P-C, Ho F-M, Kuo M-L. Cyclooxygenase-2 inducing Mcl-1-dependent survival mechanism in human lung adenocarcinoma CL1.0 cells. J Biol Chem 2001;276:48997–49002.
67. Arber N, Hibshoosh H, Yasui W, Neugut AI, Hibshoosh A, Yao Y, Sgambato A, Yamamoto H, Shapira I, Rosenman D, Fabian I, Weins I, Tahara E, Holt PR. Abnormalities in the expression of cell cycle-regulated proteins in tumors of the small bowel. Cancer Epidemiol Biomarkers Prev 1999;8:1101–1105.
68. Riverd N, Boucher M-J, Asselin C, L'Allemain G. MAP kinase cascade is required for p27 downregulation and S phase entry in fibroblasts and epithelial cells. Am J Physiol Cell Physiol 1999;277:C652–C664.

69. LaBaer J, Garrett MD, Stevenson LF, Slingerland JM, Sandhu C, Chou HS, Fattaey A, Harlow E. New functional activities for the p21 family of CDK inhibitors. Genes Dev 1997;11:847–862.
70. Hiyama H, Iavarone A, LaBaer J, Reeves SA. Regulated ectopic expression of cyclin D1 induces transcriptional activation of the cdk inhibitor p21 gene without altering cell cycle progression. Oncogene 1997;14:2533–2542.
71. Dong Y, Chi SL, Borowsky AD, Fan Y, Weiss RH. Cytosolic $p21^{Waf1/Cip1}$ increases cell cycle transit in vascular smooth muscle cells. Cell Signal 2004;16:263–269.
72. Dupont J, Karas M, LeRoith D. The cyclin-dependent kinase inhibitor $p21^{CIP/WAF}$ is a positive regulator of insulin-like growth factor I-induced cell proliferation in MCF-7 human breast cancer cells. J Biol Chem 2003;278:37256–37264.
73. Zhang C, Kavurma MM, Lai A, Khachigian LM. Ets-1 protects vascular smooth muscle cells from undergoing apoptosis by activating $p21^{WAF1/Cip1}$. J Biol Chem 2003;278:27903–27909.
74. Biankin AV, Kench JG, Morey AL, Lee C-S, Biankin SA, Head DR, Hugh TB, Henshall SM, Sutherland RL. Overexpression of $p21^{WAF1/CIP1}$ is an early event in the development of pancreatic intraepithelial neoplasia. Cancer Res 2001;61:8830–8837.
75. Rigas B, Goldman IS, Levine L. Altered eicosanoid levels in human colon cancer. J Lab Clin Med 1993;122:518–523.
76. Sheng H, Shao J, Morrow JD, Beauchamp RD, DuBois RN. Modulation of apoptosis and Bcl-2 expression by prostaglandin E_2 in human colon cancer cells. Cancer Res 1998;58:362–366.
77. Buchanan FG, Wang D, Bargiacchi F, DuBois RN. Prostaglandin E_2 regulates cell migration via the intracellular activation of the epidermal growth factor receptor. J Biol Chem 2003;278:35451–35457.
78. Pai R, Soreghan B, Szabo IL, Pavelka M, Baatar D, Tarnawski AS. Prostaglandin E_2 transactivates EGF receptor: a novel mechanism for promoting colon cancer growth and gastrointestinal hypertrophy. Nat Med 2002;8:289–293.

Received July 13, 2004. Accepted April 27, 2005.

Address requests for reprints to: Raymond N. DuBois, MD, PhD, 694 Preston Research Building, Vanderbilt-Ingram Cancer Center, Nashville, Tennessee 37232-6838. e-mail: raymond.dubois@vanderbilt.edu; fax: (615) 936-2697.

Supported in part by US Public Health Service grants DK 47297, P30CA-68485, DK 62112, and P01CA-77839 (to R.N.D.), the T.J. Martell Foundation, and the National Colorectal Cancer Research Alliance. K.K. is supported by a research fellowship from the Uehara Memorial Foundation. R.N.D. is the Hortense B. Ingram Professor of Molecular Oncology.

The authors thank Dr S.K. Dey, Dr K. Washington, Dr Joanne Brown, and Kelly Parman for kind advice and Dr T. Daikoku for help in preparing computer-generated data images.

FEBS Letters 579 (2005) 5430–5436 FEBS 29985

Hypertonic sodium chloride induction of cyclooxygenase-2 occurs independently of NF-κB and is inhibited by the glucocorticoid receptor in A549 cells

Won Chung Lim[a], Mikyung Park[a], Jae-Jun Bahn[a], Hiroyasu Inoue[b], Young Joo Lee[a,*]

[a] *College of Engineering, Institute of Biotechnology, Department of Bioscience and Biotechnology, Sejong University, Kwang-Jin-Gu, Seoul 143-747, Republic of Korea*
[b] *Department of Food Science and Nutrition, Nara Women's University, Nara, Japan*

Received 28 June 2005; revised 16 August 2005; accepted 19 August 2005

Available online 20 September 2005

Edited by Richard Marais

Abstract Cellular response to a hypertonic environment is important for fluid clearance in the lung. Hypertonicity modulates prostaglandin synthesis by influencing cyclooxygenase-2 (COX-2) expression in tissues such as liver and kidney via a mitogen-activated protein kinase (MAPK)-dependent pathway. However, little is known about COX-2 expression in response to hypertonicity in the lung. COX-2 mRNA accumulation induced by hypertonic NaCl was detected after 1 h of treatment, and COX-2 mRNA continued to accumulate until 18 h, the longest time point examined, in human alveolar epithelial A549 cells. This induction was a transcriptional event that occurred in the absence of the protein synthesis inhibitor cycloheximide and was the result of enhanced promoter activity, as examined with the use of full-length COX-2 promoter-driven reporter plasmids. The induction of COX-2 expression by hypertonic NaCl did not require the activation of NF-κB. The p38 MAPK inhibitor, SB203580, or MEK1/2 inhibitor, U0126, inhibited hypertonic induction of COX-2 expression. We examined whether the hypertonic induction of COX-2 was under the influence of glucocorticoid; we found that COX-2 promoter activity and mRNA and protein levels were depressed by dexamethasone and antagonized by the glucocorticoid receptor (GR) antagonist RU486. Our data demonstrate that the induction of COX-2 expression by hypertonic NaCl occurs independently of NF-κB and is inhibited by the GR in A549 cells.

Keywords: COX-2; Hypertonic sodium chloride; NF-κB; Glucocorticoid receptor; Alveolar epithelial cells

1. Introduction

Salt and water transport play an important role in alveolar fluid clearance (AFC), and active sodium ion transport drives osmotic water transport in the lung. The alveoli must remain open and free from fluid for efficient gas exchange to occur [1]. Intact AFC, therefore, is critical in clearing fluid from the lungs at birth and keeping the alveolar space relatively fluid-free for adequate gas exchange under physiological conditions [2–4].

One enzyme that may be involved in this process is cyclooxygenase (COX), a key regulatory enzyme in the biosynthesis of prostaglandins (PGs) from arachidonic acid [5]. COX-2 has a diverse assortment of biological functions in mammalian tissues, such as regulation of vascular tone, expression and secretion of rennin, and salt and water homeostasis in the kidneys [6]. Recent studies on the effects of salt on COX-2 expression in the kidney have identified some mechanisms for the regulation of COX-2 expression. It was reported that a low-salt medium regulates COX-2 expression by p38- and NF-κB-dependent signaling pathways in cultured cortical cells from the thick ascending limb of the loop of Henle [6,7]. Hypertonic NaCl activated COX-2 in renal medullary interstitial cells through the transactivation of the epidermal growth factor receptor [8]. Pathways involving the transcription factor NF-κB and mitogen-activated protein kinase (MAPK) play a central role in the high-salt-mediated regulation of COX-2 expression in mammalian kidney cells [9,10]. All three members of the MAPK family (ERK, JNK-2, and p38) as well as Src kinases are required for tonicity-stimulated COX-2 expression in inner medullary collecting duct cells [10].

Cellular dysfunction induced by hypertonic NaCl in alveolar epithelial cells could play an important role in the lung fluid balance under both normal and pathological conditions. Saline infusion has been reported to have a significant influence on inflammation-related gene expression in the lung [11]. Previous studies have shown that the inhibition of prostaglandin synthesis inhibits the flow of liquid from the fetal lungs [12–14]. However, the effects of hypertonic stress on COX-2 expression in alveolar epithelial cells and the mechanism involved are not known. In the present study, we examined the hypertonic NaCl induction of COX-2 expression in the human alveolar epithelial cell line A549.

2. Materials and methods

2.1. Materials

Cycloheximide, pyrrolidine dithiocarbamate (PDTC), SB203580, U0126, urea, NaCl, mannitol, 3-(5′-hydroxymethyl-2′-furyl)-1-benzylindazole (YC-1), aldosterone, spironolactone, dexamethasone, RU486, 12-*O*-tetradecanoylphorbol-13-acetate (TPA) and Dulbecco's modified Eagle's medium (DMEM)/Ham's F12 were purchased from Sigma (St. Louis, MO, USA). Fetal calf serum (FCS), Trizol Reagent, and penicillin/streptomycin were purchased from GIBCO Invitrogen (Grand Island, NY, USA).

*Corresponding author. Fax: +82 2 3408 3334.
E-mail address: yjlee@sejong.ac.kr (Y.J. Lee).

0014-5793/$30.00
doi:10.1016/j.febslet.2005.08.077

2.2. Cell culture, transfection, and luciferase assays

A549 cells, a human pulmonary epithelial cell line, were grown in DMEM/Ham's F12 nutrient mixture containing 10% FCS and penicillin/streptomycin in a humidified 37 °C incubator. COX-2-Luc, a firefly luciferase reporter construct containing the mouse COX-2 gene promoter fragment (3.4 kb), −327/+59, a firefly luciferase reporter deletion construct of the human COX-2 promoter, KBM, an NF-κB binding region site-specific mutant of −327/+59, hα ENaC-Luc, a firefly luciferase reporter construct containing the human α ENaC promoter fragment (1.4 kb), and 3 × (NF-κB)tk-Luc, a firefly luciferase reporter construct containing three repeated NF-κB-responsive elements, were kindly provided Dr. Huifang Cheng (Vanderbilt University School of Medicine, Tennessee, USA) [6], Dr. Hiroyasu Inoue (Nara Women's University, Nara, Japan) [15], Dr. Christie P. Thomas (University of Iowa College of Medicine and the Veterans Affairs Medical Center, Iowa, USA) [16], and Dr. Sam Okret (Karolinska University Hospital Huddinge, Huddinge, Sweden) [17], respectively. A549 cells were transiently transfected with COX-2-Luc, −327/+59, KBM, hα ENaC-Luc, or 3 × (NF-κB)tk-Luc by electroporation. Electroporation was performed with a Gene Pulser II (Bio-Rad, Hercules, CA, USA). Cells were trypsinized, washed in cold PBS, and resuspended in PBS. A 400 μl portion of the suspension was mixed with 20 μg of plasmid DNA.

After 5 min at room temperature, cells were pulsed at 1000 μF and 250 V. After 10 min incubation at 37 °C, the suspension was diluted in medium and cultured for 24 h. Cells were replaced with fresh medium and treated with high salt (100 mM NaCl; 200 mosmol/kgH_2O) to the normal medium resulting in final osmolarity of 500 mosmol/kgH_2O or pretreated with specific inhibitors for 30 min before treatment of high salt for 18 h. After treatment, the cells were harvested and lysed with reporter lysis buffer (Promega Luciferase Assay system). The cell extract was mixed with the luciferase assay reagent and analyzed by the luminometer (Lumat LB 9507, EG&G Berthold, Bad Widbad, Germany).

2.3. Reverse transcription-PCR

Total RNA was extracted using Trizol Reagent according to the manufacturer's instruction. RNA pellets were dissolved in diethylpyrocarbonate-treated water. The yield of RNA was quantified by spectroscopy at 260 nm. Samples were aliquoted and stored at −80 °C until further processing. To synthesize first strand cDNA, 3 μg total RNA was incubated at 70 °C for 5 min with 0.5 μg of random hexamer and deionized water (up to 11 μl). The reverse transcription (RT) reaction was performed using 40 U of M-MLV reverse transcriptase (Promega, Madison, WI, USA) in 5 × reaction buffer (250 mmol/l Tris–HCl; pH 8.3, 375 mM KCl, 15 mM $MgCl_2$, 50 mM DTT), RNase inhibitor at 1 U/μl, and 1 mM dNTP mixtures at 37 °C for 60 min. The reaction was terminated by heating at 70 °C for 10 min, followed by cooling at 4 °C. The resulting cDNA was added to the PCR mixture containing 10 × PCR buffer (100 mM Tris–HCl, pH 8.3, 500 mM KCl, 15 mM $MgCl_2$), 25 U of rTaq polymerase (TakaRa, Shiga, Japan), 4 μl of 2.5 mM dNTP mixtures, and 10 pmol of primers each. The final volume was 50 μl. Samples were amplified at 94 °C for 5 min, 23 cycles of 94 °C for 45 s, 55 °C for 45 s, and 72 °C for 45 s using Mastercycler gradient (Eppendorf, Hamburg, Germany). β-actin was amplified for 20 cycles, followed by 72 °C for 5 min. The primers used were: COX-2 sense primer, 5′-TTCAAATGAGATTGTGGGAAAATTGCT-3′; COX-2 antisense primer, 5′-AGATCATCTCTGCCTGAGTATCTTT-3′[18]; β-actin sense primer, 5′-CCTGACCCTGAAGTACCCCA-3′, β-actin antisense primer, 5′-CGTCATGCAGCTCATAGCTC-3′; IL-8 sense primer, 5′-AAGGAACCATCTCACTG-3′, IL-8 antisense primer, 5′-GATTCTTGGATACCACAGAG-3′. The expected size of amplicons for COX-2, ®-actin, and IL-8 are 305, 550, 500, and 369 bp, respectively.

2.4. Western blot analysis

Protein extracted from A549 cells was isolated in lysis buffer (150 mM NaCl, 50 mM Tris–HCl, 5 mM EDTA, 1% Nonidet P-40, 0.5% deoxycholate, 1% SDS) with protease inhibitor cocktail (Sigma) on ice for 1 h and then centrifuged for 20 min at 13 000 × *g*. Supernatant was collected and protein concentrations were measured using the Bradford method (Bio-Rad). Proteins were dissolved in sample buffer and boiled for 5 min prior to loading onto an acrylamide gel. After SDS–PAGE, proteins were transferred to a polyvinylidene difluoride membrane, blocked with 5% non-fat dry milk in Tris-buffered saline containing 0.1% Tween-20 (TBST) for 60 min at room temperature. The membranes were incubated for 2 h at room temperature with 1:1000 dilution of COX-2 polyclonal antibody (Cayman, Ann Arbor, MI, USA). Equal lane loading was assessed using β-actin monoclonal antibody (Sigma). After washing with TBST, blots were incubated with 1:5000 dilution of the horseradish peroxidase conjugated-secondary antibody (Zymed, San Francisco, CA, USA), and washed again three times with TBST. The transferred proteins were visualized with an enhanced chemiluminescence detection kit (Amersham Pharmacia Biotech, Buckinghamshire, UK).

2.5. Statistical analysis

Data were expressed as means ± S.E.M., and statistical analysis for single comparison was performed using the Student's *t* test. The criterion for statistical significance was $P < 0.05$.

3. Results

3.1. Hypertonic NaCl induces COX-2 mRNA and protein expression in A549 cells

We determined the effects of hypertonic NaCl on COX-2 expression in A549 cells by using RT-PCR and Western blot analyses. A549 cells were treated with 100 mM NaCl, 200 mM urea, or 200 mM mannitol to the normal medium resulting in final osmolarity of 500 mosmol/kgH_2O. As shown in Fig. 1A, membrane-permeable urea did not affect the COX-2 protein levels, but the membrane-impermeable agents, NaCl and mannitol, increased COX-2 protein levels in the A549 cells. This observation indicates that the induction of COX-2 regulation in A549 cells in the presence of a high salt concentration occurs in response to cell volume changes by tonicity rather than by the osmolarity of the surrounding fluid. The A549 cells were treated with hypertonic NaCl for 0, 0.5, 1, 2, 4, 6, or 18 h. COX-2 mRNA was not detected after 0 or 0.5 h of the high salt treatment, but COX-2 mRNA was detected after 1 h and continued to accumulate until 18 h. To examine whether the induction of COX-2 mRNA was the result of increased transcription from the COX-2 promoter, we performed a reporter assay using a luciferase construct containing the full-length mouse COX-2 promoter. As shown in Fig. 1C, hypertonic NaCl significantly increased the luciferase activity of the full-length COX-2 promoter in the A549 cells.

We examined whether the hypertonic NaCl induction of COX-2 gene expression requires protein synthesis by pre-treating A549 cells for 2 h with or without cycloheximide (10 μg/ml), a protein synthesis inhibitor, and then incubating the cells in the presence or absence of 100 mM NaCl for 18 h. As a positive control, we performed RT-PCR for interleukin-8 (IL-8) [19]. The increased expression of COX-2 mRNA induced by the high-salt medium was not affected by cycloheximide pretreatment (Fig. 1D), although cycloheximide alone significantly increased IL-8 mRNA in the A549 cells. This result suggests that protein synthesis is not involved and indicates that the response is elicited by pre-existing transcription factor(s), possibly by NF-κB.

3.2. Hypertonic NaCl regulation of COX-2 is not mediated by NF-κB in A549 cells

The transcription factor NF-κB is important in the hypertonic NaCl regulation of COX-2 in kidney cells [9]. The binding of activated NF-κB to the COX-2 promoter region is critical for COX-2 transcriptional activation in a number of cell types [20–22]. NF-κB is a positive regulator of COX-2 expression in macrophages and colon carcinoma cell lines

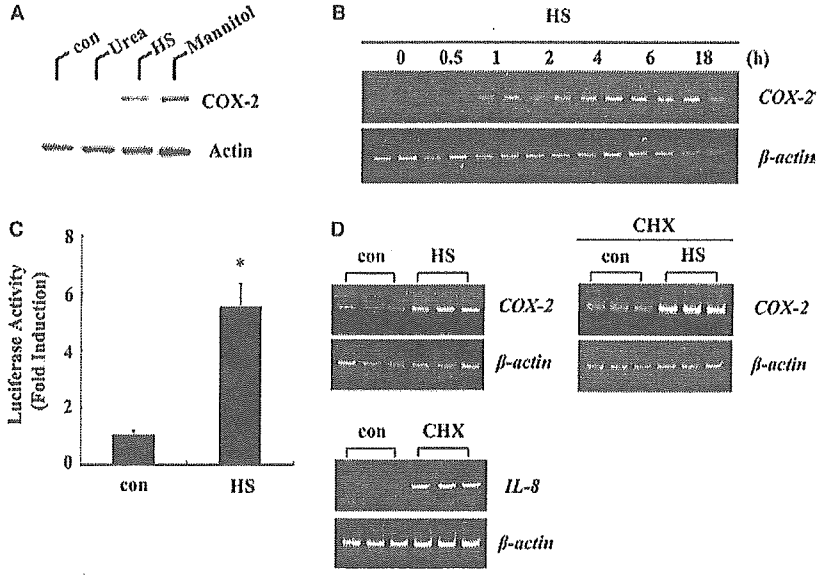

Fig. 1. Hypertonic NaCl increases COX-2 mRNA and protein expression in A549 cells. (A) A549 cells were treated with the indicated solutes (Urea, 200 mM urea; HS, 100 mM NaCl; mannitol, 200 mM mannitol) to the normal medium for 18 h. After incubation, the cell lysates were subjected to 10% SDS–PAGE and transferred to polyvinylidene difluoride membrane. Immunoblots were probed with a COX-2 antibody and reprobed with actin antibody. Bands were visualized by an ECL method, as described in Section 2. The immunoblot is representative of three independent experiments eliciting similar pattern. (B) A549 cells were treated with high salt (100 mM NaCl) for indicated time periods. Total RNA from A549 cells were analyzed for COX-2 mRNA expression by RT-PCR using specific primers as described in Section 2. Data presented are representative of two independent experiments showing similar trend. (C) A549 cells were transfected with COX-2-Luc and treated as indicated. After treatment, luciferase expression was determined as described in Section 2. Values represent the means ± S.E.M. ($N = 3$). *Represents $P < 0.05$. (D) A549 cells were pretreated with cycloheximide (10 μg/ml) for 2 h before incubation with 100 mM NaCl for 18 h. Total RNA from A549 cells were analyzed for COX-2 and IL-8 mRNA expression by RT-PCR assays. Data presented are representative of two independent experiments showing similar trend. con, untreated cells; HS, 100 mM NaCl; CHX, cycloheximide; IL-8, interleukin-8.

[23,24]. Studies have shown that IL-1β or lipopolysaccharide induces COX-2 expression via NF-κB activation in many cells including A549 cells [25–28]. To determine if NF-κB is involved in the hypertonic NaCl-induced COX-2 expression in A549 cells, we evaluated the effects of NF-κB inhibitors. We pretreated A549 cells with 5 μM MG132, a proteasome inhibitor that has been shown to prevent IκB degradation and thereby NF-κB activation [29], or 100 μM PDTC, followed by incubation in hypertonic NaCl for 18 h. As shown in Fig. 2A–C, neither MG132 nor PDTC inhibited COX-2 expression or promoter activation in cells exposed to hypertonic NaCl. No reduction in hypertonic NaCl induced COX-2 expression with MG132 or PDTC suggests that COX-2 activation occurs in the absence of NF-κB activation. Interestingly, we have consistently observed increased COX-2 protein expression with MG132 as compared with that of high salt (Fig. 2A, lanes 2 and 3). Similar results were observed in M-1 mouse cortical collecting duct cell (our unpublished results). We do not exactly understand how MG132 synergistically activates COX-2 in our model system. MG132 may activate upstream targets of hypertonic COX-2 activation by triggering other signaling transduction pathways independent of protein degradation [30].

To further determine the importance of NF-κB activation, we performed reporter assay using luciferase construct driven by the 5′-flanking region of the COX-2 promoter (−327/+59) containing NF-κB binding site. The COX-2 promoter (−327/+59) showed less than 2-fold activation in response to 100 mM NaCl (Fig. 2D). The 0.3 kb COX-2 promoter fragment with mutation at the NF-κB site (−223/−214) also had a marginal effect on luciferase expression (Fig. 2D). As a positive control for KBM, we used TPA [15]. These data suggest that NF-κB binding element is not critical in COX-2 upregulation by high salt in A549 cells. Furthermore, the hypertonic NaCl did not affect NF-κB-dependent luciferase expression in A549 cells. As a positive control for NF-κB-dependent gene transcription, we used YC-1, an activator of soluble guanylate cyclase, which initiates IKKα/β and NF-κB activation [31] (Fig. 2E). These observations indicate that NF-κB is not activated by hypertonic NaCl and imply that, although both salt and cytokines induce COX-2 expression, different signaling mechanisms exist for the hypertonic NaCl and cytokine induction of COX-2.

3.3. The hypertonic NaCl regulation of COX-2 in A549 cells is mediated by MEK1/2 and p38 MAPK

Study has shown that MAPK family members play a role in COX-2 gene expression induced by a hypertonic medium, which is crucial for cell survival under hyperosmotic shock [10]. The MAPK p38 is an essential component of the hypertonic signaling response pathway in mammals and is a major regulator in COX-2 upregulation [32–35]. To study the involvement of the MAPK pathway in the hypertonic NaCl induction of COX-2 expression in A549 cells, we evaluated the effects of p38 and MEK1/2 inhibitors on COX-2 expression. We pretreated A549 cells with SB203580 (a p38 MAPK inhibitor) or U0126 (a MEK1/2 inhibitor) for 30 min and then co-treated the cells with hypertonic NaCl for 18 h. The high-salt induction COX-2 mRNA and protein expression was

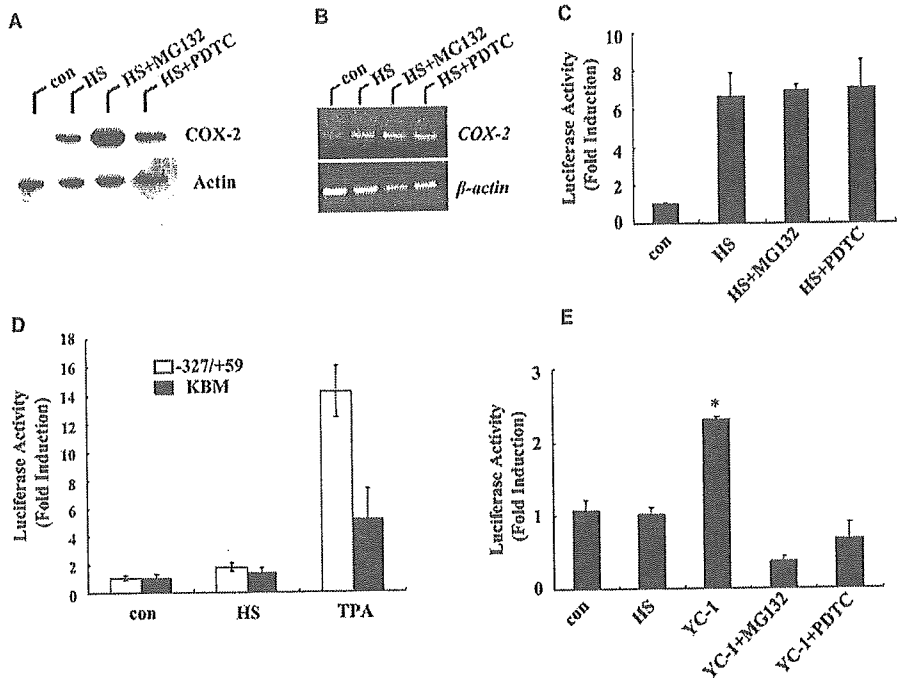

Fig. 2. NF-κB is not involved in hypertonic NaCl induction of COX-2 in A549 cells. (A) A549 cells were pretreated with PDTC (100 μM) or MG132 (5 μM) for 30 min before incubation with 100 mM NaCl for 18 h. Immunoblots were probed with a COX-2 antibody and reprobed with actin antibody, as described in Section 2. (B) A549 cells were pretreated with PDTC (100 μM) or MG132 (5 μM) for 30 min before incubation with 100 mM NaCl for 18 h. Total RNA from A549 cells were analyzed for COX-2 mRNA expression by RT-PCR assays, as described in Section 2. (C) A549 cells were transfected with COX-2-Luc and treated as indicated. After treatment, luciferase expression was determined as described in Section 2. Values represent the means ± S.E.M. ($N = 3$). (D) A549 cells were transfected with −327/+59 or KBM and treated as indicated. After treatment, luciferase expression was determined as described in Section 2. Values represent the means ± S.E.M. ($N = 3$). (E) A549 cells were transfected with the 3 × (NF-κB)tk-Luc and treated as indicated. After treatment, luciferase expression was determined. Values represent the means ± S.E.M. ($N = 3$). *Represents $P < 0.05$. con, untreated cells; HS, 100 mM NaCl. All experiments were repeated at least twice.

significantly blocked by SB203580 and U0126 (Fig. 3A and B). Furthermore, hypertonic NaCl-mediated full-length COX-2 promoter driven luciferase activity was partially inhibited by SB203580 and U0126 (Fig. 3C). It appears that p38 and MEK1/2 pathways affect not only at the level of transcription but also that of post-transcription in high-salt induction COX-2 expression in A549 cells. These results suggest that the activation of the p38 and MEK1/2 pathways is critical for the induction of COX-2 in A549 cells by a high-salt medium.

3.4. Dexamethasone inhibits hypertonic NaCl induction of COX-2 expression in A549 cells

Glucocorticoids regulate sodium uptake and fluid transport in both adult and fetal lungs, and studies have shown that a single dexamethasone injection increases AFC [36–40]. Dexamethasone suppresses COX-2 expression in the myelomonocytic leukemia cell line U937 [41]. The glucocorticoid receptor (GR) is involved in the tonic suppression of renal cortical COX-2 expression in animals [42]. To examine the possible

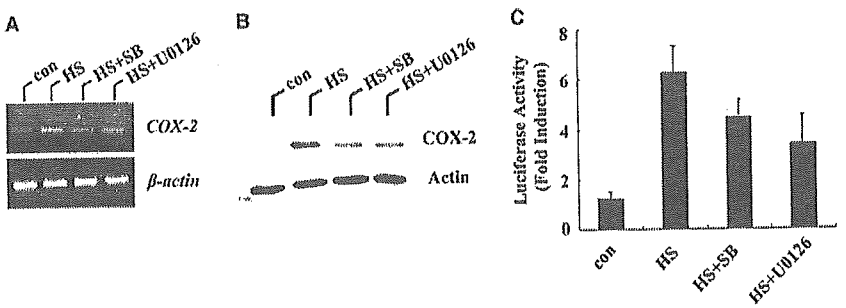

Fig. 3. MEK1/2 and p38 MAPK are involved in hypertonic NaCl induction of COX-2 in A549 cells. (A) A549 cells were pretreated with U1026 (10 μM) or SB203580 (10 μM) for 30 min before incubation with 100 mM NaCl for 18 h. Immunoblots were probed with a COX-2 antibody and reprobed with actin antibody, as described in Section 2. Data presented are representative of two independent experiments showing similar trend. (B) A549 cells were pretreated with U1026 (10 μM) or SB203580 (10 μM) for 30 min before incubation with 100 mM NaCl for 18 h. Total RNA from A549 cells were analyzed for COX-2 mRNA expression by RT-PCR assays, as described in Section 2. (C) A549 cells were transfected with COX-2-Luc and treated as indicated. After treatment, luciferase expression was determined as described in Section 2. Values represent the means ± S.E.M. ($N = 3$). con, untreated cells; HS, 100 mM NaCl; SB, SB203580. The immunoblot is representative of three independent experiments eliciting similar pattern.

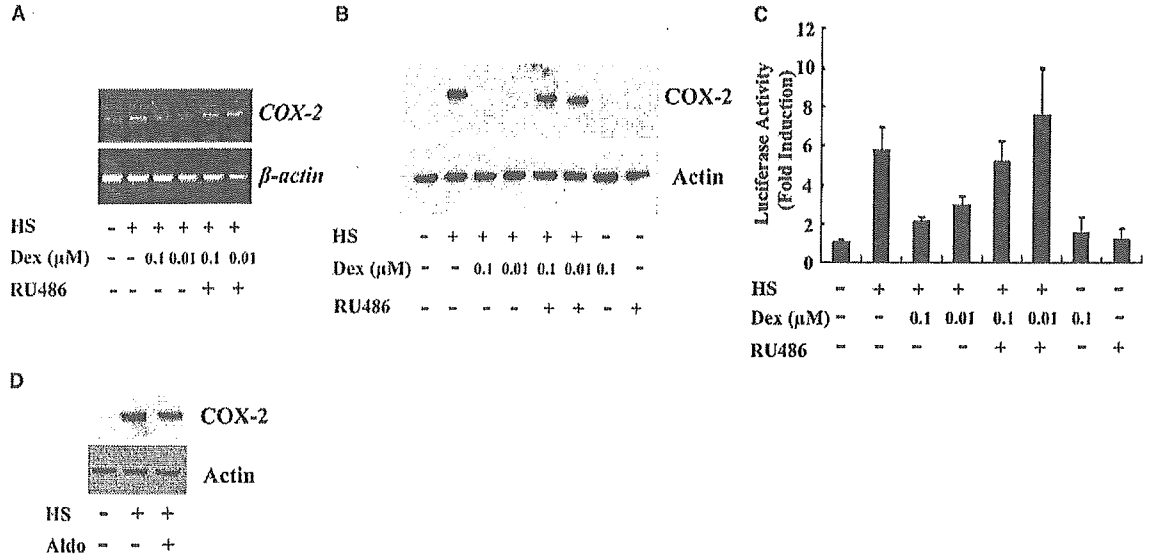

Fig. 4. Dexamethasone inhibits hypertonic NaCl induction of COX-2 in A549 cells. (A) A549 cells were pretreated with dexamethasone (0.01 or 0.1 μM) and/or RU486 (1 μM) for 1 h before incubation with 100 mM NaCl for 18 h. Total RNA from A549 cells were analyzed for COX-2 mRNA expression by RT-PCR assays, as described in Section 2. Data are representative of two independent experiments. (B) A549 cells were pretreated with dexamethasone (0.01 or 0.1 μM) and/or RU486 (1 μM) for 1 h before incubation with 100 mM NaCl for 18 h. Immunoblots were probed with a COX-2 antibody and reprobed with actin antibody, as described in Section 2. Blots are representative of four independent experiments showing similar pattern. (C) A549 cells were transfected with COX-2-Luc and treated as indicated. After treatment, luciferase expression was determined as described in Section 2. Experiments were repeated four times. (D) A549 cells were pretreated with aldosterone (0.1 μM) for 1 h before incubation with 100 mM NaCl for 18 h. Immunoblots were probed with a COX-2 antibody and reprobed with actin antibody. Blots are representative of two independent experiments showing similar pattern. Values represent the means ± S.E.M. ($N = 3$). *Represents $P < 0.05$. con, untreated cells; HS, 100 mM NaCl; Dex, dexamethasone; Aldo, aldosterone. Experiments were repeated twice.

role of the GR in the hypertonic NaCl induction of COX-2 in A549 cells, we pre-incubated cells with dexamethasone and/or the GR antagonist RU486 for 1 h and co-treated with NaCl. Neither dexamethasone nor RU486 in the absence of high salt had an effect on the COX-2 protein level or promoter activity. However, dexamethasone did block the hypertonic NaCl-induced COX-2 mRNA (Fig. 4A) and protein (Fig. 4B) expression, and COX-2 promoter activity (Fig. 4C). The suppressive effect of dexamethasone was antagonized by the GR antagonist RU486, suggesting that the response is mediated by the GR and glucocorticoid-specific. To further determine the specificity of the inhibitory effect of dexamethasone on salt-induced COX-2 regulation, we examined whether aldosterone exhibits similar suppressive effects. Cells were pre-incubated with aldosterone and/or the mineralocorticoid receptor antagonist spironolactone for 1 h and were co-treated with NaCl for 18 h. As shown in Fig. 4D, the application of aldosterone did not have an effect on the hypertonic NaCl induction of COX-2 protein expression in A549 cells. As a positive control, we performed an αENaC promoter-driven reporter gene assay; aldosterone significantly increased αENaC-dependent reporter gene transcription, and spironolactone blocked this induction (data not shown). These results indicate that dexamethasone inhibits hypertonic NaCl-induced COX-2 regulation through the GR in A549 cells.

4. Discussion

We studied the induction of COX-2 by hypertonic NaCl in lung epithelial A549 cells and observed that NaCl increases COX-2 expression at the level of transcription. Our study suggests that p38 and MEK1/2, and not NF-κB, are involved in the signal transduction leading to the expression of COX-2 induced by hypertonic NaCl. The NaCl induction of COX-2 in the lung cells could be a non-specific inflammatory-related response, but urea, a hyperosmotic agent that can promote cell lysis and can be irritating to cells, did not induce COX-2 in our study. COX-2 induction was observed in response to an increase in tonicity. The hypertonic NaCl induction of COX-2 has been studied most intensively in kidney tissue [6,7,9,10,43]. The expression of COX-2 in the kidney is tissue-specific; COX-2 is downregulated in the cortex and upregulated in the medulla [44]. Despite intensive in vivo and in vitro studies, the mechanism of the differential regulation in the kidney has not been elucidated. Our results show that hypertonic NaCl activates COX-2 expression in lung epithelial cells, as occurs in rat kidney medulla and inner medullary collecting duct cells [9,10,43].

The first candidate we investigated as a transcription factor responsible for COX-2 gene activation in lung epithelial cells was NF-κB. Studies have previously shown that hypertonic stress activates an NF-κB-COX-2-linked survival mechanism in renal medullary interstitial cells [43]. Other studies have shown that the inhibition of glycogen synthase kinase-3β protects renal cells from hypertonic stress via the induction of the NF-κB-COX-2-dependent pathway [9]. However, in contrast to the situation in the kidney medulla, the hypertonic activation of COX-2 in lung epithelial cells was not dependent on NF-κB. In addition, it appears that part of the signal transduction pathway leading to COX-2 activation is shared but is not identical with other stimuli, such as LPS and cytokines. The NaCl induction of COX-2 was inhibited by a glucocorticoid,

which agrees with the observations made in other studies of LPS and cytokines [45–47], while dexamethasone suppressed LPS- and IL-1β-induced COX-2 regulation in a NF-κB-dependent manner. Recent studies have shown that the inhibition of granulocyte-macrophage colony-stimulating factor by dexamethasone is independent of NF-κB [48,49], and the inhibition of NF-κB cannot account for all the repressive effects of dexamethasone on inflammatory genes such as COX-2 [50]. The transcription factor involved in the hypertonic NaCl activation of COX-2 remains to be identified, but it is most likely a pre-existing protein(s) rather than a newly synthesized protein, as shown by the cycloheximide experiments. It is possible that the factor is specific to the lung; however, we have observed the hypertonic NaCl activation of COX-2 in other cells, such as vascular smooth muscle (data not shown), which indicates that the response is not restricted to lung and kidney tissues. A few transcription factors activated by hypertonicity are known. One well-known example is tonicity-responsive enhancer (TonE) binding protein (TonEBP). TonEBP is a member of the Rel family of transcriptional activators that include NF-κB and nuclear factor of activated T cells [51]. Studies have previously shown that the hypertonic induction of COX-2 mRNA is not reduced by the expression of DN-TonEBP [52]. However, additional studies are needed to confirm that the hypertonic induction of COX-2 is independent of TonEBP. The identification of the transcription factor responsible for the hypertonic NaCl induction of COX-2 would greatly enhance our understanding of the hypertonicity-triggered signal transduction pathway that leads to COX-2 activation.

Acknowledgements: This work has been supported by grants from the Korean Ministry of Health and Welfare (01-PJ1-PG1-01CH06-0003) and BK21 program to Y.J.L.

References

[1] Matalon, S., Lazrak, A., Jain, L. and Eaton, D.C. (2002) Invited review: biophysical properties of sodium channels in lung alveolar epithelial cells. J. Appl. Physiol. 93, 1852–1859.
[2] O'Brodovich, H. (1991) Epithelial ion transport in the fetal and perinatal lung. Am. J. Physiol. Cell Physiol. 261, C555–C564.
[3] Matthay, M.A. and Wiener-Kronish, J.P. (1990) Intact epithelial barrier function is critical for the resolution of alveolar edema in humans. Am. Rev. Respir. Dis. 142, 1250–1257.
[4] Ware, L.B. and Matthay, M.A. (2001) Alveolar fluid clearance is impaired in the majority of patients with acute lung injury and the acute respiratory distress syndrome. Am. J. Respir. Crit. Care Med. 163, 1376–1383.
[5] Needleman, P., Turk, J., Jakschik, B.A., Morrison, A.R. and Lefkowith, J.B. (1986) Arachidonic acid metabolism. Annu. Rev. Biochem. 55, 69–102.
[6] Cheng, H.F. and Harris, R.C. (2002) Cyclooxygenase-2 expression in cultured cortical thick ascending limb of Henle increases in response to decreased extracellular ionic content by both transcriptional and post-transcriptional mechanisms. Role of p38-mediated pathways. J. Biol. Chem. 277, 45638–45643.
[7] Cheng, H.F., Wang, J.L., Zhang, M.Z., McKanna, J.A. and Harris, R.C. (2000) Role of p38 in the regulation of renal cortical cyclooxygenase-2 expression by extracellular chloride. J. Clin. Invest. 106, 681–688.
[8] Zhao, H., Tian, W., Tai, C. and Cohen, D.M. (2003) Hypertonic induction of COX-2 expression in renal medullary epithelial cells requires transactivation of the EGFR. Am. J. Physiol. Renal Physiol. 285, F281–F288.
[9] Rao, R., Hao, C.M. and Breyer, M.D. (2004) Hypertonic stress activates glycogen synthase kinase 3beta-mediated apoptosis of renal medullary interstitial cells, suppressing an NFkappaB-driven cyclooxygenase-2-dependent survival pathway. J. Biol. Chem. 279, 3949–3955.
[10] Yang, T., Huang, Y., Heasley, L.E., Berl, T., Schnermann, J.B. and Briggs, J.P. (2000) MAPK mediation of hypertonicity-stimulated cyclooxygenase-2 expression in renal medullary collecting duct cells. J. Biol. Chem. 275, 23281–23286.
[11] Sabbadini, M., Barisani, D., Conforti, E., Marozzi, A., Ginelli, E., Miserocchi, G. and Meneveri, R. (2003) Gene expression analysis in interstitial lung edema induced by saline infusion. Biochim. Biophys. Acta 1638, 149–156.
[12] Wlodek, M.E., Harding, R. and Thorburn, G.D. (1994) Effects of inhibition of prostaglandin synthesis on flow and composition of fetal urine, lung liquid, and swallowed fluid in sheep. Am. J. Obstet. Gynecol. 170, 186–195.
[13] Cassin, S. (1984) Effect of indomethacin on fetal lung liquid formation. Can. J. Physiol. Pharmacol. 62, 157–159.
[14] Stevenson, K.M. and Lumbers, E.R. (1992) Effects of indomethacin on fetal renal function, renal and umbilicoplacental blood flow and lung liquid production. J. Dev. Physiol. 7, 257–264.
[15] Huang, W.C., Chen, J.J., Inoue, H. and Chen, C.C. (2003) Tyrosine phosphorylation of I-kappa B kinase alpha/beta by protein kinase C-dependent c-Src activation is involved in TNF-alpha-induced cyclooxygenase-2 expression. J. Immunol. 170, 4767–4775.
[16] Mick, V.E., Itani, O.A., Loftus, R.W., Husted, R.F., Schmidt, T.J. and Thomas, C.P. (2001) The alpha-subunit of the epithelial sodium channel is an aldosterone-induced transcript in mammalian collecting ducts, and this transcriptional response is mediated via distinct *cis*-elements in the 5′-flanking region of the gene. Mol. Endocrinol. 15, 575–588.
[17] Bladh, L.G., Liden, J., Dahlman-Wright, K., Reimers, M., Nilsson, S. and Okret, S. (2005) Identification of endogenous glucocorticoid repressed genes differentially regulated by a glucocorticoid receptor mutant able to separate between nuclear factor-{kappa}B and activator protein-1 repression. Mol. Pharmacol. 67, 815–826.
[18] Hla, T. and Neilson, K. (1992) Human cyclooxygenase-2 cDNA. Proc. Natl. Acad. Sci. USA 89, 7384–7388.
[19] Van Wetering, S., Mannesse-Lazeroms, S.P., Van Sterkenburg, M.A., Daha, M.R., Dijkman, J.H. and Hiemstra, P.S. (1997) Effect of defensins on interleukin-8 synthesis in airway epithelial cells. Am. J. Physiol. Lung Cell. Mol. Physiol. 272, L888–L896.
[20] Deng, W.G., Zhu, Y. and Wu, K.K. (2003) Up-regulation of p300 binding and p50 acetylation in tumor necrosis factor-alpha-induced cyclooxygenase-2 promoter activation. J. Biol. Chem. 278, 4770–4777.
[21] Hwang, D., Jang, B.C., Yu, G. and Boudreau, M. (1997) Expression of mitogen-inducible cyclooxygenase induced by lipopolysaccharide: mediation through both mitogen-activated protein kinase and NF-kappaB signaling pathways in macrophages. Biochem. Pharmacol. 54, 87–96.
[22] Newton, R., Kuitert, L.M., Bergmann, M., Adcock, I.M. and Barnes, P.J. (1997) Evidence for involvement of NF-kappaB in the transcriptional control of COX-2 gene expression by IL-1beta. Biochem. Biophys. Res. Commun. 237, 28–32.
[23] D'Acquisto, F., Iuvone, T., Rombola, L., Sautebin, L., Di Rosa, M. and Carnuccio, R. (1997) Involvement of NF-kappaB in the regulation of cyclooxygenase-2 protein expression in LPS-stimulated J774 macrophages. FEBS Lett. 418, 175–178.
[24] Kojima, M., Morisaki, T., Izuhara, K., Uchiyama, A., Matsunari, Y., Katano, M. and Tanaka, M. (2000) Lipopolysaccharide increases cyclo-oxygenase-2 expression in a colon carcinoma cell line through nuclear factor-kappa B activation. Oncogene 19, 1225–1231.
[25] Luo, S.F., Wang, C.C., Chien, C.S., Hsiao, L.D. and Yang, C.M. (2003) Induction of cyclooxygenase-2 by lipopolysaccharide in canine tracheal smooth muscle cells: involvement of p42/p44 and p38 mitogen-activated protein kinases and nuclear factor-kappaB pathways. Cell. Signal. 15, 497–509.
[26] Yang, C.M., Chien, C.S., Hsiao, L.D., Luo, S.F. and Wang, C.C. (2002) Interleukin-1beta-induced cyclooxygenase-2 expression is mediated through activation of p42/44 and p38 MAPKS, and NF-kappaB pathways in canine tracheal smooth muscle cells. Cell. Signal. 14, 899–911.
[27] Catley, M.C., Chivers, J.E., Cambridge, L.M., Holden, N., Slater, D.M., Staples, K.J., Bergmann, M.W., Loser, P., Barnes, P.J. and Newton, R. (2003) IL-1beta-dependent activation of NF-kappaB

mediates PGE2 release via the expression of cyclooxygenase-2 and microsomal prostaglandin E synthase. FEBS Lett. 547, 75–79.
[28] Wissink, S., van Heerde, E.C., vand der Burg, B. and van der Saag, P.T. (1998) A dual mechanism mediates repression of NF-kappaB activity by glucocorticoids. Mol. Endocrinol. 12, 355–363.
[29] Traenckner, E.B., Wilk, S. and Baeuerle, P.A. (1994) A proteasome inhibitor prevents activation of NF-kappa B and stabilizes a newly phosphorylated form of I kappa B-alpha that is still bound to NF-kappa B. EMBO J. 13, 5433–5441.
[30] Wu, H.M., Wen, H.C. and Lin, W.W. (2002) Proteasome inhibitors stimulate interleukin-8 expression via Ras and apoptosis signal-regulating kinase-dependent extracellular signal-related kinase and c-Jun N-terminal kinase activation. Am. J. Respir. Cell Mol. Biol. 27, 234–243.
[31] Chang, M.S., Lee, W.S., Chen, B.C., Sheu, J.R. and Lin, C.H. (2004) YC-1-induced cyclooxygenase-2 expression is mediated by cGMP-dependent activations of Ras, phosphoinositide-3-OH-kinase, Akt, and nuclear factor-kappaB in human pulmonary epithelial cells. Mol. Pharmacol. 66, 561–571.
[32] Sheikh-Hamad, D. and Gustin, M.C. (2004) MAP kinases and the adaptive response to hypertonicity: functional preservation from yeast to mammals. Am. J. Physiol. Renal Physiol. 287, F1102–F1110.
[33] Ridley, S.H., Dean, J.L., Sarsfield, S.J., Brook, M., Clark, A.R. and Saklatvala, J.A. (1998) p38 MAP kinase inhibitor regulates stability of interleukin-1-induced cyclooxygenase-2 mRNA. FEBS Lett. 439, 75–80.
[34] Dean, J.L., Brook, M., Clark, A.R. and Saklatvala, J. (1999) p38 mitogen-activated protein kinase regulates cyclooxygenase-2 mRNA stability and transcription in lipopolysaccharide-treated human monocytes. J. Biol. Chem. 274, 264–269.
[35] Uhlik, M.T., Abell, A.N., Johnson, N.L., Sun, W., Cuevas, B.D., Lobel-Rice, K.E., Horne, E.A., Dell'Acqua, M.L. and Johnson, G.L. (2003) Rac-MEKK3-MKK3 scaffolding for p38 MAPK activation during hyperosmotic shock. Nat. Cell Biol. 5, 1104–1110.
[36] Barquin, N., Ciccolella, D.E., Ridge, K.M. and Sznajder, J.I. (1997) Dexamethasone upregulates the Na-K-ATPase in rat alveolar epithelial cells. Am. J. Physiol. Lung Cell. Mol. Physiol. 273, L825–L830.
[37] Ingbar, D.H., Duvick, S., Savick, S.K., Schellhase, D.E., Detterding, R., Jamieson, J.D. and Shannon, J.M. (1997) Developmental changes of fetal rat lung Na-K-ATPase after maternal treatment with dexamethasone. Am. J. Physiol. Lung Cell. Mol. Physiol. 272, L665–L672.
[38] Renard, S., Voilley, N., Bassilana, F., Lazdunski, M. and Barbry, P. (1995) Localization and regulation by steroids of the alpha, beta and gamma subunits of the amiloride-sensitive Na+ channel in colon, lung and kidney. Pflugers Arch. 430, 299–307.
[39] Tchepichev, S., Ueda, J., Canessa, C., Rossier, B.C. and O'Brodovich, H. (1995) Lung epithelial Na channel subunits are differentially regulated during development and by steroids. Am. J. Physiol. Cell Physiol. 269, C805–C812.
[40] Noda, M., Suzuki, S., Tsubochi, H., Sugita, M., Maeda, S., Kobayashi, S., Kubo, H. and Kondo, T. (2003) Single dexamethasone injection increases alveolar fluid clearance in adult rats. Crit. Care Med. 31, 1183–1189.
[41] Inoue, H. and Tanabe, T. (1998) Transcriptional role of the nuclear factor kappa B site in the induction by lipopolysaccharide and suppression by dexamethasone of cyclooxygenase-2 in U937 cells. Biochem. Biophys. Res. Commun. 244, 143–148.
[42] Zhang, M.Z., Harris, R.C. and McKanna, J.A. (1999) Regulation of cyclooxygenase-2 (COX-2) in rat renal cortex by adrenal glucocorticoids and mineralocorticoids. Proc. Natl. Acad. Sci. USA 96, 15280–15285.
[43] Hao, C.M., Yull, F., Blackwell, T., Komhoff, M., Davis, L.S. and Breyer, M.D. (2000) Dehydration activates an NF-kappaB-driven, COX2-dependent survival mechanism in renal medullary interstitial cells. J. Clin. Invest. 106, 973–982.
[44] Yang, T., Singh, I., Pham, H., Sun, D., Smart, A., Schnermann, J.B. and Briggs, J.P. (1998) Regulation of cyclooxygenase expression in the kidney by dietary salt intake. Am. J. Physiol. Renal Physiol. 274, F481–F489.
[45] Inoue, H., Umesono, K., Nishimori, T., Hirata, Y. and Tanabe, T. (1999) Glucocorticoid-mediated suppression of the promoter activity of the cyclooxygenase-2 gene is modulated by expression of its receptor in vascular endothelial cells. Biochem. Biophys. Res. Commun. 254, 292–298.
[46] Newton, R., Seybold, J., Kuitert, L.M., Bergmann, M. and Barnes, P.J. (1998) Repression of cyclooxygenase-2 and prostaglandin E2 release by dexamethasone occurs by transcriptional and post-transcriptional mechanisms involving loss of polyadenylated mRNA. J. Biol. Chem. 273, 32312–32321.
[47] Wang, Z. and Tai, H.H. (1998) Interleukin-1 beta and dexamethasone regulate gene expression of prostaglandin H synthase-2 via the NF-κB pathway in human amnion derived WISH cells. Prostaglandins Leukot. Essent. Fatty Acids 59, 63–69.
[48] Bergmann, M.W., Staples, K.J., Barnes, P.J. and Newton, R. (2004) Nuclear factor-kappaB does not mediate the inhibitory effects of dexamethasone on granulocyte-macrophage colony-stimulating factor expression. Immunology 111, 430–434.
[49] Bergmann, M.W., Staples, K.J., Smith, S.J., Barnes, P.J. and Newton, R. (2004) Glucocorticoid inhibition of granulocyte macrophage-colony-stimulating factor from T cells is independent of control by nuclear factor-kappaB and conserved lymphokine element 0. Am. J. Respir. Cell Mol. Biol. 30, 555–563.
[50] Chivers, J.E., Cambridge, L.M., Catley, M.C., Mak, J.C., Donnelly, L.E., Barnes, P.J. and Newton, R. (2004) Differential effects of RU486 reveal distinct mechanisms for glucocorticoid repression of prostaglandin E release. Eur. J. Biochem. 271, 4042–4052.
[51] Miyakawa, H., Woo, S.K., Dahl, S.C., Handler, J.S. and Kwon, H.M. (1999) Tonicity-responsive enhancer binding protein, a rel-like protein that stimulates transcription in response to hypertonicity. Proc. Natl. Acad. Sci. USA 96, 2538–2542.
[52] Woo, S.K., Lee, S.D., Na, K.Y., Park, W.K. and Kwon, H.M. (2002) TonEBP/NFAT5 stimulates transcription of HSP70 in response to hypertonicity. Mol. Cell Biol. 22, 5753–5760.

Heparanase Is Involved in Angiogenesis in Esophageal Cancer through Induction of Cyclooxygenase-2

Takaomi Okawa,[1] Yoshio Naomoto,[1] Tetsuji Nobuhisa,[1] Munenori Takaoka,[1] Takayuki Motoki,[1] Yasuhiro Shirakawa,[1] Tomoki Yamatsuji,[1] Hiroyasu Inoue,[4] Mamoru Ouchida,[2] Mehmet Gunduz,[3] Motowo Nakajima,[5] and Noriaki Tanaka[1]

Abstract **Purpose:** Both heparanase and cyclooxygenase-2 (COX-2) are thought to play critical roles for tumor malignancy, including angiogenesis, although it is unknown about their relationship with each other in cancer progression. We hypothesized that they may link to each other on tumor angiogenesis.

Experimental Design: The expressions of heparanase and COX-2 in 77 primary human esophageal cancer tissues were assessed by immunohistochemistry to do statistical analysis for the correlation between their clinicopathologic features, microvessel density, and survival of those clinical cases. Human esophageal cancer cells were transduced with heparanase cDNA and used for reverse transcription-PCR and Western blot to determine the expression of heparanase and COX-2. COX-2 promoter vector and its deletion/mutation constructs were also used along with transduction of heparanase cDNA for luciferase assay.

Results: Heparanase and COX-2 protein expression exhibited a similar pattern in esophageal tumor tissues, and their expression correlated with tumor malignancy and poor survival. Their expression also revealed a significant correlation with high intratumoral microvessel density. Up-regulation of COX-2 mRNA and protein was observed in esophageal cancer cells transfected with heparanase cDNA. COX-2 promoter was activated after heparanase cDNA was transduced and the deletion/mutation of three transcription factor (cyclic AMP response element, nuclear factor-κB, and nuclear factor-interleukin-6) binding elements in COX-2 promoter strongly suppressed its activity.

Conclusion: Our results suggest that heparanase may play a novel role for COX-2-mediated tumor angiogenesis.

Two essential processes required for metastasis are neoangiogenesis and tumor cell invasion of the basement membrane and extracellular matrix (1). Heparanase specifically cleaves carbohydrate chains of heparan sulfate proteoglycans (HSPG) present in the extracellular matrix and on the cell surface (2). Heparanase has been identified in highly invasive normal and malignant cells, including cytotrophoblasts, activated cells of the immune system, and lymphoma, melanoma, and carcinoma cells (2–8). Normal physiologic functions of heparanase are related to embryonic morphogenesis, wound healing, tissue repair, and inflammation. Enhanced heparanase expression has been reported to correlate with the metastatic potential of human tumor cells (3, 4, 7, 8) and shorter postoperative survival of patients with various cancers (9–12).

Cyclooxygenase-2 (COX-2) is a rate-limiting enzyme involved in the conversion of arachidonic acid to prostaglandin H_2, the precursor of various molecules, including prostaglandins, prostacyclins, and thromboxanes. COX-2 is known to contribute to tumorigenesis and the malignant phenotype of tumor cells in various ways, including (*a*) inhibition of apoptosis (13), (*b*) increased angiogenesis (14), (*c*) increased invasiveness (15, 16), (*d*) modulation of inflammation and immunosuppression (17), and (*e*) conversion of procarcinogens to carcinogens (18, 19). COX-2 converts arachidonic acid to prostaglandins and induces angiogenic factors, such as vascular endothelial growth factor and basic fibroblast growth factor (FGF; refs. 14, 20), and selective inhibitors of COX-2 are effective in inhibition of cancer growth (14, 21). On the other hand, heparanase may also contribute to angiogenesis by cleaving HSPGs and releasing angiogenic factors, such as basic FGF, vascular endothelial growth factor, heparin growth factor, platelet-derived growth factor, and transforming growth factor-β (3, 22–25). Therefore, these two molecules are thought to play

Authors' Affiliations: Departments of [1]Gastroenterological Surgery, Transplant, and Surgical Oncology, [2]Molecular Genetics, and [3]Oral Pathology and Medicine, Graduate School of Medicine and Dentistry, Okayama University, Okayama, Japan; [4]National Cardiovascular Center Research Institute, Osaka, Japan; and [5]Novartis Pharma Tsukuba Institute, Tsukuba, Japan

Received 5/18/05; revised 7/28/05; accepted 8/15/05.

Grant support: Ministry of Education, Culture, Sports, Science, and Technology, Japan grant 13671306.

The costs of publication of this article were defrayed in part by the payment of page charges. This article must therefore be hereby marked *advertisement* in accordance with 18 U.S.C. Section 1734 solely to indicate this fact.

Requests for reprints: Yoshio Naomoto, Department of Gastroenterological Surgery, Transplant, and Surgical Oncology, Graduate School of Medicine and Dentistry, Okayama University, 2-5-1 Shikatacho, Okayama 700-8558, Japan. Phone: 81-86-235-7257; Fax: 81-86-221-8775; E-mail: ynaomoto@md.okayama-u.ac.jp.

doi:10.1158/1078-0432.CCR-05-1103

a critical role in controlling the invasion and metastasis of malignant tumors. However, the relationship between heparanase and COX-2 has not yet been elucidated.

Esophageal squamous cell carcinoma (ESCC) remains one of the most aggressive malignant tumors, and its prognosis remains worse than those of other gastrointestinal malignancies. The clinical outlook for patients with ESCC is still very poor due to the high rate of local and distant metastasis (26–28). Although conventional pathologic assessment has served as the standard estimation of prognosis of patients with ESCC, it does not always define the individual risk of recurrence after surgical resection. Tumor cell invasion and secondary spread to the blood and lymph vessels are the hallmarks of malignant disease and the greatest impediment to cancer therapy. Recent advances in the molecular genetics of ESCC have stimulated attempts to evaluate the prognostic relevance of specific molecular alterations in the tumor. Identification of a prognostic marker susceptible to or modifiable by direct therapeutic intervention will result in therapeutic and prognostic improvements for these patients.

The present study was designed to map the distribution of heparanase and COX-2 in human esophageal carcinoma using immunohistochemical staining and define the relationship between heparanase/COX-2 and clinicopathologic features. Our findings suggested a positive relationship between heparanase and COX-2 expression, and we therefore elucidated the relationship between heparanase and COX-2 in terms of signal transduction. We attempted to identify transcription factors and transcriptional regulatory elements located in the COX-2 promoter that is activated by heparanase. Based on the additional evidence thus obtained, we propose that the expression of the *COX-2* gene might be regulated by heparanase. This invokes a dynamic relationship with tumor angiogenesis.

Materials and Methods

Patients and tissue sampling. We examined 77 ESCCs, including mucosal carcinomas (n = 6) and submucosal carcinomas (n = 24), obtained from 77 previously untreated patients. The patients included 72 men and 5 women with a mean age of 68.3 years (range, 38-79 years). Tissue samples were surgically resected at the Department of Surgery, Keiyukai Hospital (Sapporo, Hokkaido, Japan) in 1994. Two experienced pathologists, who were blinded to the clinical data and results of other diagnostic tests, determined the grade of dysplasia in all lesions. The clinicopathologic characteristics were evaluated according to the guidelines of the Union Internationale Contre le Cancer. The study protocol was approved by the Human Ethics Review Committee of Okayama University Graduate School of Medicine and Dentistry, and a signed consent form was obtained from each subject.

Cell culture. We used three types of human ESCC cell lines and colon cancer cell lines. Three ESCC cell lines, TE1, TE6, and TE8, were obtained from the Japanese Cancer Research Resource Bank, and T.Tn was obtained from the Japan Cell Research Bank (Ibaraki, Japan). RPMI4788, colon cancer cell line, was kindly provided by the RPMI (Buffalo, NY; ref. 29). These cell lines were propagated in monolayer culture in RPMI 1640 with 25 mmol/L HEPES, 10% FCS, 100 units/mL penicillin, and 100 mg/mL streptomycin at 37°C in a humidified atmosphere of 95% air and 5% CO_2.

Monoclonal antibodies. Anti-human mouse heparanase monoclonal antibody was obtained from Novartis Pharma Tsukuba Institute (Tsukuba, Japan); the monoclonal antibody reacted with both the 65-kDa proform and the 50-kDa mature form of the human heparanase as described previously (9, 30). Monoclonal antibody 13H14 for COX-2 was obtained from IBL (Gunma, Japan). Clone F8/86 for factor VIII-related antigen/von Willebrand factor Ab-2 was obtained from Neo-Markers (Fremont, CA). Antibody for human heparanase was diluted at 1:500. 13H14 was used at a concentration of 3 μg/L and F8/86 was ready to use.

Immunohistochemistry. COX-2 and factor VIII stainings were done using formalin-fixed, paraffin-embedded serial sections. Sections (5 μm thick) were mounted on silanized slides (DAKO Japan Co., Tokyo, Japan), deparaffinized in xylene for 20 minutes, and rehydrated in graded ethanol solutions. Endogenous peroxidase was blocked by incubating the sections in 3.0% H_2O_2 in methanol for 15 minutes. For heparanase and COX-2 staining, antigen retrieval in paraffin sections was done once and thrice, respectively, by heating in 10 mmol/L citrate buffer solution (pH 6.0) in a microwave for 5 minutes. For factor VIII staining, antigen retrieval was done by pepsin (Pepsin solution, Nichirei, Tokyo, Japan) at 37°C for 15 minutes. After blocking of nonspecific reactivity with rabbit serum for 10 minutes at room temperature (Histofine SAB PO kit, Nichirei), sections were incubated overnight at 4°C with the anti-heparanase and anti-COX-2 antibody and for 1 hour at 37°C with anti-factor VIII antibody. Identification of the distribution of the primary antibody was achieved by subsequent application of a biotinylated anti-primary antibody (Histofine SAB PO kit) and streptavidin peroxidase (Histofine SAB PO kit). Immunostaining was developed using 3,3′-diaminobenzidine/H_2O_2 solution (Histofine 3,3′-Diaminobenzidine Substrate kit, Nichirei), and sections were counterstained with Mayer's hematoxylin. As a negative control, some sections were subjected to normal serum blocking and omission of the primary antibody. In each lesion, assessment of heparanase was based on the nuclear or cytoplasmic staining pattern. Assessment of COX-2 was based on the cytoplasmic staining pattern. Expressions of heparanase and COX-2 were considered positive when it stained at the invasive front and tumor edge and was present in >10% of tumor cells. Assessment of factor VIII was based on the expression in vascular endothelial cells.

Evaluation of microvessel density. Evaluation of microvessel density (MVD) was done as described previously (31). Briefly, after microscopic screening for tumor areas of highest MVD at a magnification of ×40, the vessels in five areas with the highest MVD were counted under ×200 magnification by two independent observers blinded to the patient's background. The mean value of the vessel count in five fields by the two observers was considered the MVD for the tumor. Generally, there was no significant interobserver difference, and in cases with wide differences, MVDs were reevaluated by a third observer until the three observers reached a consensus.

Analysis of the relationship between heparanase expression and clinicopathologic factors. Heparanase and COX-2 immunostaining was detected in the cytoplasm of cancer cells. We analyzed the interaction between heparanase/COX-2 expression and clinicopathologic characteristics and evaluated it as a prognostic factor for esophageal cancer patients.

Plasmids and oligonucleotides. Human heparanase cDNA was kindly provided by Dr. Motowo Nakajima (Novartis Pharma Tsukuba Institute), the characteristics of which were described previously (30, 32). Luciferase constructs with the COX-2 promoter (−1,432/+59, −327/+59, −220/+59, −124/+59, −52/+59, KBM, ILM, CRM, KBM-ILM, ILM-CRM, CRM-KBM, and CRM-ILM-KBM) were kind gifts from Dr. Hiroyuki Inoue (National Cardiovascular Center Research Institute, Osaka, Japan; ref. 33). pCRE-Luc, which contains four tandem copies of the nuclear factor-κB (NF-κB) consensus sequence fused to a TATA-like promoter, and pNF-κB-Luc, which contains multiple copies of the cyclic AMP response element (CRE) binding sequence fused to a TATA-like promoter, were purchased from BD Biosciences (San Jose, CA; Mercury Pathway Profiling Luciferase System). pRL-tk, the control luciferase plasmid, was purchased from Promega (Madison, WI).

Transfection. The 3,726-bp-long cDNA coding human *heparanase* gene was inserted into an expression vector, pBK-cytomegalovirus (Stratagene, La Jolla, CA), and directly used for transfection of ESCC cell

lines by LipofectAMINE 2000 reagent (Life Technologies, Gaithersburg, MD). Cells were transfected with 1 μg plasmid DNA in the presence of 10 μL LipofectAMINE 2000 in six-well tissue culture plates containing Opti-MEM reduced-serum medium (Life Technologies). After a 5-hour incubation, the medium was replaced with fresh RPMI 1640 supplemented with 10% fetal bovine serum, 2 mmol/L L-glutamine, 100 units/mL penicillin, and 100 mg/mL streptomycin. For Western blotting, cells were seeded at a density of 2×10^5 per well in six-well dishes and grown to 80% confluence. For each well, plasmid (4 μg; human heparanase cDNA) was introduced into cells using 10 μg LipofectAMINE 2000 according to the manufacturer's instructions. After 12 hours of incubation, the medium was replaced with basal medium. For the luciferase assay, cells were seeded at a density of 5×10^4 per well in 24-well dishes and grown to 50% to 60% confluence. For each well, plasmid DNA (1.0 μg; human heparanase/mock and COX-2 reporter plasmids) was introduced into cells using 3 μg LipofectAMINE 2000 according to the manufacturer's instructions. Luciferase activity was measured in cellular extracts as described below.

Reverse transcription-PCR. Total RNA was isolated from cells using RNAzol (Cinna Biotecx, Friendswood, TX) in a single-step phenol extraction method and used as a template. Reverse transcription was done at 22°C for 10 minutes and then at 42°C for 20 minutes, and PCR was done with specific primers in a volume of 50 μL according to the manufacturer's protocol (PCR kit; Perkin-Elmer/Cetus, Norwalk, CT). The following specific primers were used: heparanase sense (5′-TTCGATCCCAAGGAATCAAC-3′) and antisense (5′-GTAGTGATGCCATGTAACTGAATC-3′), COX-2 sense (5′-GGGTTGCTGGGGGAAGAAATGTG-3′) and antisense (5′-GGTGGCTGTTTTGGTAGGCTGTG-3′), and glyceraldehyde-3-phosphate dehydrogenase sense (5′-CAGCCGAGCCACATC-3′) and antisense (5′-TGAGGCTGTTGTCATACTTCT-3′). For heparanase, the amplification reaction involved denaturation at 95°C for 45 seconds, annealing at 60°C for 1 minute, and extension at 72°C for 1 minute; for COX-2, the amplification reaction involved denaturation at 94°C for 45 seconds, annealing at 60°C for 45 seconds, and extension at 72°C for 1 minute using a thermal cycler (Perkin-Elmer, Foster City, CA). The PCR products were applied on 1% agarose gels and visualized by SYBR Gold (Molecular Probes, Eugene, OR) staining.

Quantitative real-time reverse transcription-PCR. Heparanase mRNA copy number in cell lines was determined by quantitative real-time reverse transcription-PCR using a LightCycler instrument and a LightCycler DNA Master SYBR Green I kit (Roche Molecular Biochemicals, Indianapolis, IN). Amplifications were done in glass capillary tubes using 20 μL reaction containing 3 mmol/L $MgCl_2$, 0.5 μmol/L of each primer, and 2 μL of 10× LightCycler FastStart DNA Master SYBR Green I. PCR amplification began with a 60-second denaturation step at 95°C followed by 40 cycles of denaturation at 95°C for 15 seconds, annealing at 58°C for 10 seconds, and extension at 72°C for 9 seconds. The oligonucleotides used as specific primers were 5′-GCGGTTACCCTATCCTTTTT-3′ and 5′-GCAGCAACTTTGGCATTTC-3′. Copy numbers of mRNA were calculated from serially diluted standard curves generated from purified cDNA template, which consisted of a human heparanase cDNA of 1,758 bp inserted into the expression vector. Data analysis was done using LightCycler Software (Roche Molecular Biochemicals).

Western blotting. Cells were collected by trypsinization and washed twice in cold PBS. Cells then were dissolved in lysis buffer containing 20 mmol/L Tris-HCl (pH 7.6), 150 mmol/L NaCl, 1 mmol/L $CaCl_2$, 1 mmol/L $MgCl_2$, 1% NP40, 10% glycerol, and protease inhibitors (1 mmol/L phenylmethylsulfonyl fluoride, 1 mmol/L DTT, 20 μg/mL aprotinin, and 20 μmol/L leupeptin). Lysis was carried out at 4°C for 30 minutes and lysates were centrifuged at 15,000 rpm for 20 minutes. The protein concentration of the supernatant was determined using the Bio-Rad Protein Assay (Bio-Rad, Hercules, CA). Equal amounts (40 μg) of proteins were electrophoresed under reducing conditions on 12% (w/v) polyacrylamide gels. Proteins were electrophoretically transferred to Hybond polyvinylidene difluoride transfer membranes (Amersham, Arlington Heights, IL) and incubated with primary antibodies against COX-2 and heparanase and then peroxidase-linked secondary antibody. An Amersham Enhanced Chemiluminescence Western System (Amersham, Tokyo, Japan) was used to detect secondary probes.

Luciferase assay. Reporter plasmids containing the 327-bp flanking region of the human COX-2 promoter with deletion or site-specific mutation are represented schematically in Fig. 5A and B. Relative positions of the NF-κB site, nuclear factor-interleukin-6 (NF-IL6) site, and the CRE are indicated. Heparanase cDNA expression vector was transiently transfected with each reporter plasmid together with pRL-tk used as an internal control for the Dual-Luciferase Reporter Assay System (Promega). The cells were then harvested, lysed, and assayed for luciferase activity. Luciferase activity was measured by Luminoskan (Labsystems, Helsinki, Finland). Results are represented as relative luciferase activities normalized by dividing with the luciferase activity using the empty vector (mock). Data are mean ± SD of four individual experiments.

Statistical analysis. Heparanase expression was assessed for association with clinicopathologic variables and COX-2 expression using the χ^2 two-tailed test, Fisher's exact test, and Spearman's correlation coefficient test. Survival analysis was calculated using the Kaplan-Meier method and compared by the Wilcoxon test. $P < 0.05$ denotes the presence of a statistically significant difference. Differences of MVD between heparanase-positive and heparanase-negative tumors were examined using the unpaired t test. The rate of double-stained cells was assessed using the two-tailed test.

Results

Distribution of heparanase and cyclooxygenase-2 in normal and cancer tissues of the esophagus. Heparanase was barely detectable in normal esophageal tissue (34, 35). However, in the stromal compartment adjacent to tumor tissue, vascular endothelial cells and fibroblasts as well as inflammatory cells, such as macrophages, lymphocytes, and neutrophils, stained strongly for heparanase (Fig. 1A and B). Heparanase expression was also observed in dysplastic areas. Severe and moderate dysplasia was associated with stronger heparanase expression than that seen in mild dysplasia as we have shown previously (35). With respect to invasive tumors, heparanase and COX-2 were expressed in the cytoplasm and cell surface of carcinoma cells at the tumor edge and invasive front, respectively (Fig. 1B and D). Heparanase exhibited progressively stronger expression in lesions from dysplasia through invasive cancer of the esophagus. Metastatic lymph nodes had less or an equal level of heparanase expression in comparison with their primary lesions (35).

COX-2 staining was not detected in normal esophageal tissues (data not shown). Inflammatory cells and vascular endothelial cells in stromal tissue adjacent to tumor tissues showed strong COX-2 expression similar to the pattern observed for heparanase (Fig. 1C and D). In addition, COX-2 expression in esophageal carcinomas was evident as the cells progressed from dysplasia to invasive squamous carcinoma (data not shown). In advanced cancer tissues, COX-2 protein immunoreactivity was diffusely present in the cytoplasm. COX-2 expression exhibited a very similar pattern to that of heparanase expression in esophageal cancer tissues (Fig. 1C and D).

Relationship between heparanase/cyclooxygenase-2 expression and clinicopathologic factors. Because COX-2 and heparanase have been known as bad prognostic markers in various cancers due to their contribution to cancer invasion and metastasis, and the current similar expression pattern in our samples was

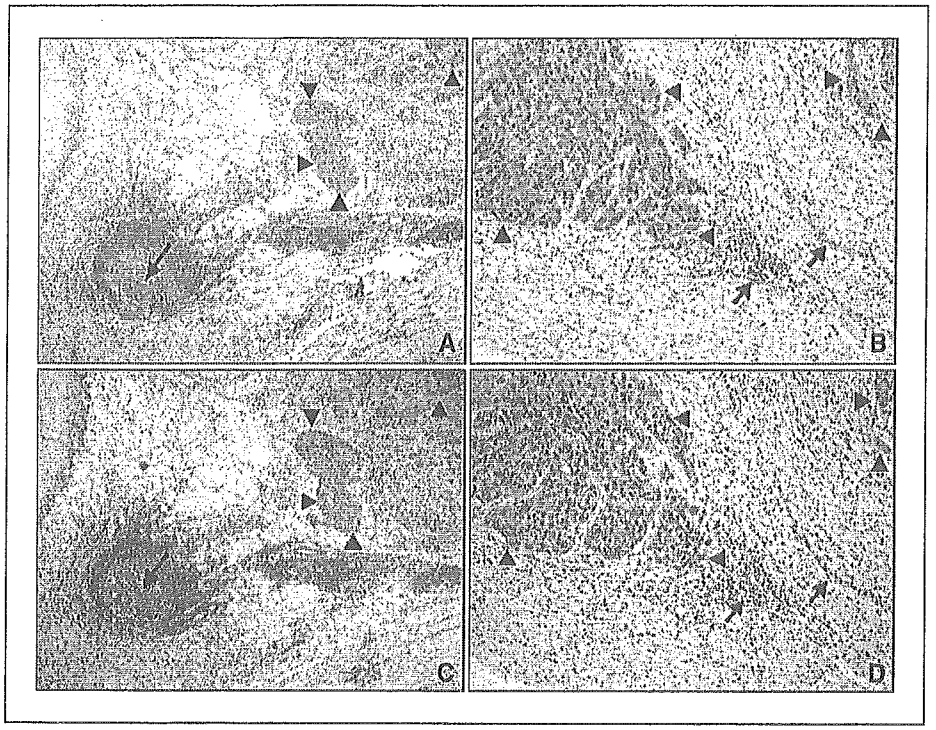

Fig. 1. Immunohistochemical analysis of the heparanase (*A* and *B*) and COX-2 (*C* and *D*) proteins in esophageal tissues. Stromal tissues around tumor tissue are both heparanase and COX-2 positive (*A* and *C*, respectively), whereas neither heparanase nor COX-2 was expressed in normal epithelium. Strong staining of heparanase and COX-2 was also detected at the invasive front in cancer tissue (*B* and *D*, respectively). Original magnifications, ×200 (*A* and *C*) and ×400 (*B* and *D*). Tumor cells at the invasive front were strongly stained with heparanase and COX-2 (*A-D, arrowheads*). Inflammatory cells (*B* and *D*) and the cells in the lymph follicle (*A* and *C*) were also stained with heparanase and COX-2 (*arrows*).

observed, we examined such relationship of both molecules in the same samples. Figure 2A-D shows immunohistochemical analysis for heparanase and COX-2. Figure 2A and C shows positive analysis for heparanase and COX-2, and Fig. 2B and D shows negative analysis for heparanase and COX-2. Fifty-three of the 77 (68.8%) ESCC cases stained positively for heparanase and 56 of 77 (72.7%) stained positively for COX-2. The relationship between heparanase/COX-2 expression and clinicopathologic characteristics is shown in Table 1. With respect to depth of invasion, all cases of carcinoma *in situ* were heparanase negative. Heparanase and COX-2 immunoreactivity increased gradually from T_1 to T_4 stage tumors. All T_4 lesions were both heparanase positive and COX-2 positive. Both heparanase and COX-2 were correlated significantly with invasion depth (P = 0.0018 and 0.0209, respectively). Thirty-two of 40 (80.0%) tumors with lymph node metastasis were positive for heparanase expression, and heparanase was negative in 16 of 37 (43.2%) tumors without lymph node involvement (P = 0.0278). COX-2 expression was also significantly correlated to lymph node metastasis (P = 0.0453). Of the tumors with lymph node metastasis, 32 cases were positive for both heparanase and COX-2. Heparanase staining gradually increased from stage 0 to 4 (P = 0.0406). Of the stage IV tumors, 70.0% exhibited positive staining, whereas only 1 of 5 (20%) was positive for heparanase at stage 0. Heparanase and COX-2 were detected in 31 cases of 36 (86.1%) tumors with lymphatic invasion, and 19 of 41 (46.3%) and 16 (40.2%) of 41 tumors without lymphatic invasion were negative for heparanase and COX-2, respectively (P = 0.0029 and 0.00202, respectively). Of the tumors with lymphatic invasion, 27 cases were positive for both heparanase and COX-2. These results suggest that both heparanase and COX-2 expressions in ESCC are closely involved in tumor invasion and metastasis.

We examined the survival in relation to heparanase and COX-2 expression. Seventy-five percent and 76.2% of patients with tumors negative for heparanase and COX-2, respectively, survived, whereas the survival rate was 33.7% and 35.7% in patients with heparanase and COX-2 immunopositivity 5 years after surgery (P = 0.0005 and 0.0009, respectively; Fig. 2E).

Expression of heparanase and cyclooxygenase-2 predicts neovascularization of esophageal cancer. Microvessels in tumor tissue were detected by immunohistochemical analysis using anti-factor VIII antibody. Figure 3C shows microvessels in tumor tissue. Heparanase and COX-2 were expressed in microvessels in tumor tissue (Fig. 3A and B, respectively). The MVD in the esophageal cancers ranged from 0 to 34.8 (18.6 ± 8.6, mean ± SD). Based on the mean value of the MVD for all tumors, esophageal cancers were divided into two groups: high MVD group (MVD ≥ 18.6; n = 43) and low MVD group (MVD < 18.6; n = 34; Table 2A). The number of the patients who showed high MVD was significantly associated with heparanase positive and COX-2 positive tumors (P = 0.0001 and 0.0002, respectively). Heparanase-positive tumors had a significantly higher vascularity (MVD 21.4 ± 6.5) compared with heparanase-negative tumors (MVD, 12.2 ± 7.9; P < 0.0001; Table 2B). Tumors with positive COX-2 expression also had a significantly higher MVD (20.9 ± 6.7) compared with those negative for COX-2 (12.2 ± 8.3; P < 0.0001; Table 2B). Combination of heparanase-positive and COX-2-positive expression was also significantly associated with higher MVD (Fig. 3D). The high MVD group exhibited a significantly worse survival rate (33.3%) than the low MVD group (P = 0.0021; Fig. 3E).

Comparison of heparanase and cyclooxygenase-2 expression. In both superficial carcinomas and advanced ESCCs, COX-2 expression correlated significantly with heparanase expression (Table 2C). Fifteen of 29 (51.7%) cases with early-stage cancers

were negative for both COX-2 and heparanase. On the other hand, of advanced tumors (stage T_2-T_4), 41 of 48 (85.4%) cases were positive for both COX-2 and heparanase. Interestingly, in this study, no cases were found to be heparanase positive and COX-2 negative. All of the heparanase-positive cases were also COX-2 positive. In addition, 3 of 77 (3.9%) cases were heparanase negative but COX-2 positive. These findings suggested that heparanase is strongly linked to COX-2 expression.

Heparanase up-regulates cyclooxygenase-2 mRNA and protein in human esophageal cancer cells. To analyze the relationship between heparanase and COX-2, we first examined heparanase and COX-2 protein expression by Western blotting in three ESCC cell lines (TE1, TE8, and T.Tn). All cell lines showed low-level heparanase protein expression (Fig. 4A, *lanes 1, 4,* and *7*). COX-2 protein was also showed a low expression in these cell lines. The mRNA levels of both genes were also low in all cell lines (Fig. 4B, *lane 1* for T.Tn; data not shown for TE1 and TE8). Therefore, we transfected the heparanase cDNA expression vector into the cell lines and confirmed that the heparanase mRNA and protein showed an increased expression (Fig. 4A, *lanes 3, 6,* and *9*; Fig. 4B, *lane 3*). Notably, we found that the COX-2 mRNA and protein were enhanced in the heparanase-transfected cell lines compared with the empty vector (mock)–transfected cells and parental cell lines, although COX-1 expression was not changed by heparanase (Fig. 4A and B). When we used RPMI4788, a colon cancer cell line that exhibited lower-level COX-2 expression and no heparanase expression, an increased COX-2 mRNA in the heparanase-transfected RPMI4788 cells was detected (Fig. 4B, *lane 6*). Furthermore, the increase of the COX-2 gene expression was confirmed in the T.Tn cells by real-time PCR (Fig. 4C) after transfection of the heparanase expression vector. These data suggest that the COX-2 expression is up-regulated through the heparanase induction

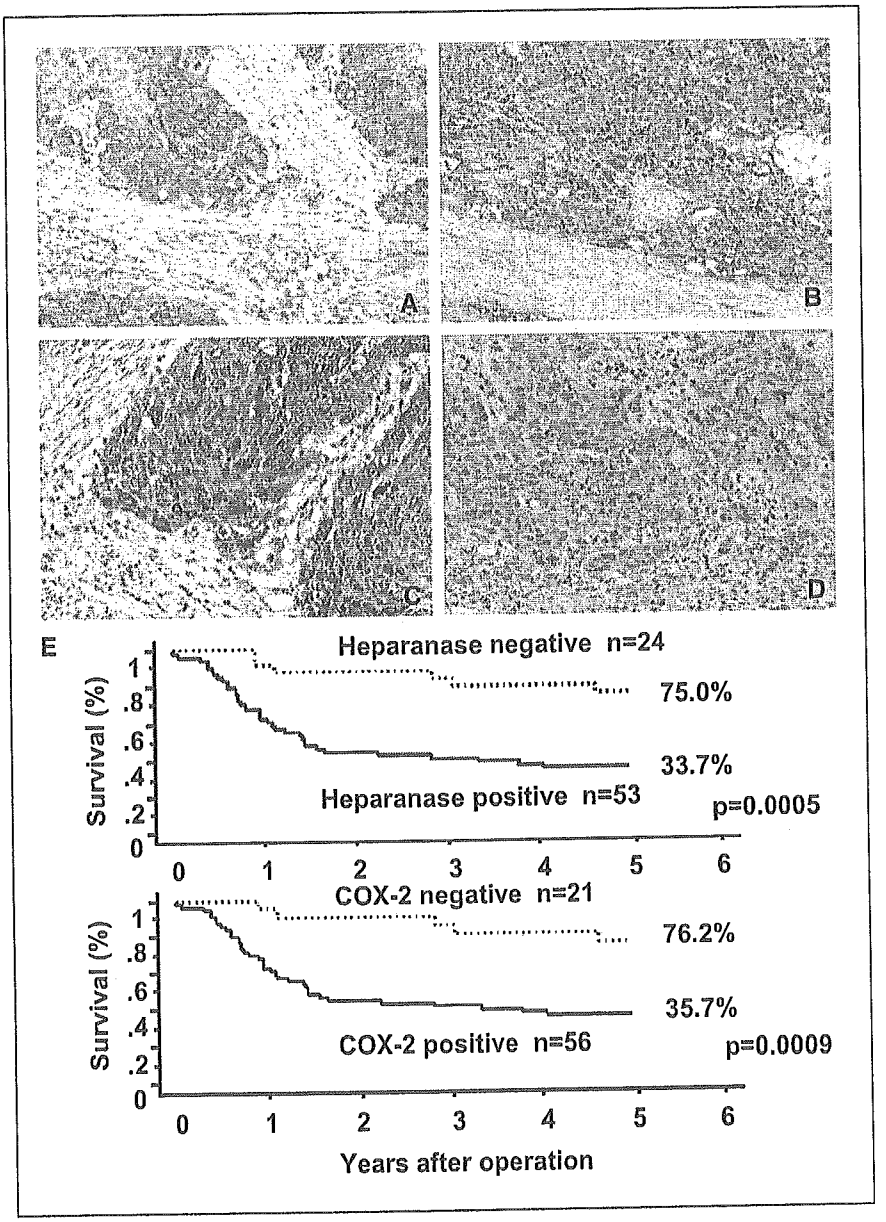

Fig. 2. Intracellular heparanase and COX-2 staining patterns in tumor cells (*A-D*). Positive staining for heparanase (*A*) and COX-2 (*C*) in the cytoplasm. Negative staining for heparanase (*B*) and COX-2 (*D*) in the cytoplasm. Original magnification, ×400. *E*, Kaplan-Meier survival curves of patients with esophageal carcinomas with respect to heparanase or COX-2 expression status. Both heparanase-positive patients and COX-2-positive patients exhibit significantly poorer survival rates compared with each group of patients who are negative.

Table 1. Relationship between heparanase or COX-2 expression and clinicopathologic variables in ESCCs

	Heparanase			COX-2		
	Negative	Positive	*P*	Negative	Positive	*P*
Differentiation						
Well	9	31	0.128	7	33	0.072
Moderate	14	18		13	19	
Poor	1	4		1	4	
Depth						
T_{is}	3	0	0.0018	2	1	0.0209
T_{1a}	2	1		2	1	
T_{1b}	12	12		11	13	
T_2	1	11		1	11	
T_3	6	25		5	26	
T_4	0	4		0	4	
Lymph node metastasis						
N_0	16	21	0.0278	14	23	0.0453
N_1	8	32		7	33	
Distant metastasis						
M_0	21	46	0.89	18	49	0.88
M_{1a}	3	5		3	5	
M_{1b}	0	2		0	2	
Stage						
0	4	1	0.0406	3	2	0.0652
I	8	7		8	7	
IIa	4	11		3	12	
IIb	3	11		2	12	
III	2	16		2	16	
IVa	2	5		2	5	
IVb	1	2		1	2	
Lymph vessel invasion						
(−)	19	22	0.0029	16	25	0.0202
(+)	5	31		5	31	
Vascular invasion						
(−)	24	47	0.169	21	50	0.181
(+)	0	6		0	6	

NOTE: (−) and (+), absence and presence, respectively, of lymph and vascular invasions.

in esophageal cancer cell lines. We further examined the gene regulation using a COX-2 promoter luciferase construct (36, 37). After cotransfection of luciferase reporter plasmid containing the longest promoter (−1,432 to +59) of the *COX-2* gene with the heparanase cDNA expression vector or empty vector (mock), the heparanase-transfected TE1, TE8, T.Tn, and RPMI4788 cells exhibited 1.87-, 1.85-, 1.74-, and 2.56-fold increases in luciferase activity compared with mock, respectively (Fig. 4D).

Identification of the cyclooxygenase-2 promoter region regulated by human heparanase. Based on earlier reports about the COX-2 transcriptional mechanism (33, 38), we hypothesized that heparanase might regulate the *COX-2* gene at the transcriptional level and that the *COX-2* is a downstream target gene of heparanase. To test this hypothesis, we used RPMI4788 cell line to analyze the heparanase-responsible regions on the COX-2 promoter. We did cotransfection of heparanase expression vector with a series of luciferase reporter plasmids that have the COX-2 promoter, encompassing the regions of −327 to +59, −220 to +59, −124 to +59, and −52 to +59 (Fig. 5A). The −327 to +59, −224 to +59, and −124 to +59 promoter regions showed 2.23-, 2.25-, and 3.28-fold increases of luciferase activity in RPMI4788 cells, respectively. However, the −52 to +59 COX-2 promoter exhibited less luciferase activity (Fig. 5B, *lanes 1-4*). Using TE8 cell line, the heparanase response pattern of the COX-2 promoter was similar to that of RPMI4788 cells, whereas the luciferase activities were low (Fig. 5B, *lanes 5-8*).

Furthermore, to define the responsible elements for heparanase in the COX-2 promoter, we used mutant forms (mNF-κB, mNF-IL6, and mCRE) of NF-κB, NF-IL6, and CRE binding elements on the COX-2 promoter containing −327 to +59 region (Fig. 6A). As shown in Fig. 6C, mNF-κB, mNF-IL6, and mCRE exhibited 2.44-, 2.16-, and 2.57-fold luciferase activity, respectively. These activities were almost same as that of the normal promoter containing −327 to +59 region (*lane1*; 2.47-fold). Next, we used double-mutant COX-2 promoter plasmids, which are mNF-κB/mCRE, mNF-κB/mNF-IL6, and mNF-IL6/